Characterising Bicyclist Posture in Various Bicycle Types for Safety Evaluation

Maria Oikonomou, Johan Iraeus, Athanasios Lioras, Vasileios Mylonas, Lambros Rorris, Athanassios Mihailidis

Abstract The growing use of bicycles and the increasing frequency of accidents underscore the need for an in-depth investigation into bicyclists' kinematics and injuries. This study aims to collect and analyse bicyclists' posture data across three bicycle types to facilitate the positioning of Human Body Model (HBM) for implementation in crash simulations. Ten male volunteers, with characteristics similar to the 50th percentile male, were measured while riding in the city, racing, and mountain bikes.

Characteristic angles of the volunteers' postures were calculated for each bicycle and for pedal angles ranging from 0 degrees to 360 degrees, with a 30-degree increment. This approach allowed for the examination of posture variations throughout the pedaling cycle and across different bicycle types. The findings indicate that, apart from the characteristic angles of the lower extremities, the pelvis and spine were most influenced through the pedaling for each bike. Notably, the differences in characteristic angles across the three bikes were greater in the pelvis, spine region, and upper extremities compared to those occurring in the lower extremities.

The posture information obtained from this study can guide the future positioning of HBMs, thereby enhancing the accuracy of crash simulations.

Keywords Bicyclist, posture, volunteer measurements, vulnerable road user, Human Body Models.

I. INTRODUCTION

Data from the European Road Safety Observatory for 2021–2022 indicate that cyclists are the sole road user group where fatalities have not declined since 2010. In 2019, more than 2,000 road deaths among cyclists in Europe were reported by police, with the proportion of serious injuries in crashes involving cyclists rising from 7% in 2010 to 9% in 2019 [1]. Therefore, further exploration of bicyclists' safety is highly important.

Investigating bicyclists' kinematics and injuries involves analysing experimental field data, as referenced in [2-3], or conducting crash simulations, as discussed below. In crash simulation, the bicyclists are often represented using human multibody models, crash test dummy models, or finite element human body models (FE-HBMs). These simulations enable exploration of various parameters influential to the injury risk. For instance, some studies examine the effects of collision speed on the cyclists' kinematics and resulting injuries [4-7], while others investigate the influence of collision angle [4-8]. Additionally, numerous publications undertake the examination of various vehicle parameters, including vehicle type [5-7][9-11], vehicle speed [3][7-10], and vehicle mass [3]. Similarly, attention is paid to various factors related to bicycles, such as bicycle type [12], bicycle speed [3][7], bicycle mass [3], rider's protection [3][4], rider's posture [9], and pedals' position [4][10]. Moreover, multiple comparative analyses of cyclists' kinematics and injury patterns with varying attributes, such as size and sex [9-11][13], or comparisons between cyclists using different two-wheelers [9][11-12], and even contrasts between cyclists' and pedestrians' kinematics and injury patterns [5-6][10], are frequently conducted across various studies. However, none of these studies reports sufficient data to define bicyclist posture, relying instead on a presumed posture that may not accurately reflect real-world conditions.

While existing research has explored various aspects of bicyclist safety, there remains a notable gap in understanding bicyclist posture, its variability, and the implications for bicyclist safety. Therefore, the objective of this study is to provide input on bicyclist posture at different pedal angles and across three different bicycle

M. Oikonomou (e-mail: oikonommg@meng.auth.gr; tel: +30 6949095907) is a PhD student and A. Mihailidis is an Emeritus Professor at School of Mechanical Engineering in Aristotle University of Thessaloniki, Greece. J. Iraeus is a Researcher at the Division of Vehicle Safety, Chalmers University of Technology in Gothenburg, Sweden. A. Lioras is a Senior Supervisor in Software Research and Development Department of BETA CAE Systems SA, in Thessaloniki, Greece. V. Mylonas is a MSc student at School of Physical Education and Sport Science in Aristotle University of Thessaloniki. L. Rorris is a Senior Manager in Software Research and Development Department of BETA CAE Systems International, Luzern, Switzerland.

types for safety evaluation. As first step, this study focuses on the subpopulation representing the average male anthropometry (50th percentile male). This information can later be utilised to position HBMs and conduct crash simulations, which will provide valuable insights to inform the development of more effective safety measures and interventions, thereby advancing the current understanding of bicyclist safety.

II. METHODS

The posture data were collected through volunteer experiments and recorded using a photogrammetric method. A detailed description of the utilised methods is provided below in six subsections. The subsections include the experimental data collection, the identification of measurements per pedal angle, the consideration of marker dimensions and skinfold thicknesses, and the calculation of joint positions, characteristic angles, and average postures.

Experimental Data Collection

Ten participants were enrolled in the study. They were selected based on height and weight criteria, consistent with the average male specifications outlined in [14]. The target values for height and weight were set at 175 cm and 77 kg, respectively. The participants' body dimensions, ranging from 171 cm to 179 cm in height and 71 kg to 80 kg in weight, were measured using a stadiometer with 1 mm accuracy and an electronic scale with a precision of 0.01 kg. None of the participants reported any pre-measurement issues related to spinal column or balance. All participants had previous experience of bikes. Ethical approval for the study was obtained from the Research Ethics and Deontology Committee of Aristotle University of Thessaloniki, under protocol number 255513/2023. All participants provided informed consent prior to participation.

Each participant was measured while riding three distinct types of bicycle, each with varying distances between the handlebar, saddle, and pedals. This approach aimed to incorporate different bike geometries that were assumed to prompt different bicyclist postures. The selected bicycle types included city, racing, and mountain bikes, as depicted in Fig. 1. It was assumed that studying these three types would be beneficial for gaining insight into different postures adopted by a broad spectrum of bicyclists. The appropriate saddle height is relative to the bicyclist's seated height, so the saddle height of each bicycle was readjusted for each participant through a bike fitting process. The participant placed his heel on the pedal while riding the bike, then pedaled backward until reaching the lowest pedal position. If the knee was fully extended in this position, the saddle height was considered correct. Due to this readjustment, the saddle-to-handlebar, and the saddle-to-pedals distances varied for each subject, forming different geometric triangles between the handlebar, saddle, and pedals points.

The saddle point was considered at the saddle base (SAb), the handlebar at the medial point between the right and left handlebar ends (HB), and the pedals at the midpoint of pedals rotation axis (PEc), as depicted in Figure A1 of the Appendix. For the city bike, the handlebar-to-pedals distance equals 814mm, while the saddle-to-handlebar and saddle-to-pedals distances range from 535mm to 542mm and from 535mm to 614mm, respectively. For the racing bike, the handlebar-to-pedals distance amounts 829mm, with the saddle-to-handlebar ranging from 740mm to 757mm, and the saddle-to-pedals ranging from 573mm to 648mm. For the mountain bike, the handlebar-to-pedals distance equals 731mm, while the saddle-to-handlebar and saddle-to-pedals range from 605mm to 612mm and from 492mm to 548mm, respectively. The geometric triangles formed between the handlebar, saddle, and pedals points for the different participants and each bike can be seen in Figure A2 of the Appendix.

Fig. 1. Measuring process of a volunteer riding the city (left), racing (middle), and mountain (right) bike.

The measurement procedure was performed at the Biomechanics Laboratory at the School of Physical Education and Sport Science of Aristotle University of Thessaloniki. Two experienced operators were involved in the measurement procedure to ensure the accuracy of data collection. The measuring system used was the Qualisys Track Manager (version 2023.1), which included 8 Miqus M3 cameras with a sampling frequency of 300 Hz and a resolution of 1824x1080 pixels. This system enabled the calculation of the centre location of reflective markers. Following the photogrammetric measurements, skinfold thickness was measured at each marker location using a caliper with a precision of 1 mm. The skinfold measurements were conducted while the participant was still seated on the city bicycle.

For the photogrammetric measurements, 52 spherical reflective markers were placed on the skin over the anatomical landmarks identified through palpation by one of the two operators. These anatomical landmarks were selected based on the recommendations of the International Society of Biomechanics (ISB) [15-16] and were considered characteristic points of the human body, used to document the human posture. It is important to note that while the selection was guided by ISB recommendations, the exact anatomical points used were not identical to those specified by the ISB, due to the small distance between some landmarks making marker recognition by the system difficult. Seven markers were positioned on the volunteer's head, 14 on the arms, four on the scapulae, two on the clavicles, four on the hips, 14 on the legs, and seven on the spine. An illustration of a subject with markers placed on his skin is presented in Fig. A3 of the Appendix, while Table AI of the Appendix contains a description of the exact location of each marker. Additionally, 12 spherical markers were placed on each bike to gather data on the bicycle's geometry and 3D position, including two markers on the axis of each wheel, three on the handlebars, two on the pedals, two on the pedal's rotation axis, and one on the saddle. The locations of these markers are depicted in Fig. A4 of the Appendix.

The measuring procedure included the following sequential steps. Initially, markers were attached to the three bicycles. These remained in place throughout the measurement session, for all participant measurements, to ensure consistency across participants. This approach guaranteed that the exact same bike points were measured for all participants, despite any adjustments of the bike, particularly the saddle height, resulting from the bike fitting process. Subsequently, the wheels of the first bicycle were securely arranged in a bike trainer equipment to maintain stability. Using the bike trainer, a medium bike resistance level (3rd out of 7) was set for all participants and all bikes. Then, markers were placed on the volunteer's anatomical landmarks, and the bicycle's saddle height was modified according to the volunteer's seated height. Once preparations were complete, the volunteer rode the bike and, in case they had slipped off the anatomical landmarks position due to skin movement, the markers were reapplied. The participant started biking for an initial period of 10 seconds, before a 20-second video capturing the participant's biking motion was recorded. After the captured video, the participant stopped biking. This approach ensured that the recorded data corresponded to typical riding postures, excluding initial acceleration or braking phases. The duration of the video was crucial for capturing multiple pedal strokes completed by the participant, enabling the extraction of posture information at various pedal angles. Participants were instructed to maintain a low biking speed, look straight ahead, and keep their hands placed on the handlebar with fingers on the brakes. After completing the biking session, the participant dismounted the bike without removing his markers. The current bicycle was removed from the bike trainer, and the next one was arranged to repeat the measuring process.

Data Selection Methodology

To ensure the accurate determination of bicyclist posture, a thorough approach was employed. The 20-second video was divided into individual frames, allowing for precise analysis. For each participant and analysed pedal angle, the most precise video frame was consistently identified. The analysed pedal angles ranged from 0° to 360°, in 30° increments. Specifically, the pedal angle of 0° was defined where the right pedal reached its highest position while the left pedal was at its lowest position. Similarly, the 90° pedal angle was determined by the right pedal being at its most forward position and the left pedal at its most backward position.

Data from each participant on each bicycle were analysed individually. To check the reliability of the data, successive markers were connected to form segment lengths. It was assumed that these segment lengths should remain constant throughout the biking movement, with only minor variations occurring due to skin movement during cycling. A total of 65 segment lengths were defined, including 24 on the upper extremities, 14 on the lower extremities, and 27 on the head and pelvis. For each video frame, the 65 segment lengths were calculated, and the mean value for each segment was determined. The frames were then grouped based on their corresponding pedal angle. Subsequently, the frames corresponding to each analysed pedal angle were compared against the

mean segment lengths. For each pedal angle, the frame with the minimum overall square difference between its calculated segment lengths and the mean segment lengths was the one used to derive the posture of the current participant. Thus, for each analysed pedal angle, one frame per participant was used.

A separate methodology was applied to check the reliability of the data for the spine region due to its unique characteristics. In this region, markers were placed on the skin on top of the spinous processes of the C7, T4, T7, T10, T12, L3, and L5 vertebrae. However, as spinal column changes curvature during cycling, it would be inaccurate to assume constant segment lengths between vertebrae. Thus, to ensure at least the correct order of the spine markers along the vertical direction, markers were verified to be arranged in a sequential manner where the Z-value decreased from C7 to L5 vertebrae.

Projecting the Markers' Measurements to the Bony Structure

The Qualisys software provides data about the centre location of the spherical reflective markers, rather than participants' bone structure, which is preferred when positioning HBMs. To obtain measurements representative of the participants' bones, two series of modifications were conducted. First, the measured data were adjusted to represent the participants' skin by subtracting the dimensions of the markers (the sum of marker radius and base height). Subsequently, a second modification was performed on the newly calculated skin data to represent the underlying bone structures. This was achieved by subtracting the skinfold thickness measured at each anatomical landmark of the volunteers.

For joints such as the elbow, wrist, knee, and ankle, characterised by two markers positioned on their lateral and medial sides, it was assumed that the participant's skin and bones align linearly with the markers' centre location. Therefore, both the markers' dimensions and skinfold thickness were subtracted in alignment with the assumed rotation axis. In scapula and shoulder region, where three markers were situated, a plane was formed between them. For the two markers placed on the scapula's spine and scapula's inferior angle, it was assumed that the participant's skin and bones were perpendicular to the formed plane at the corresponding marker's position. For the third marker placed on the shoulder, the corresponding participant's skin and bone points were assumed to be located along the vertical axis. For the trochanter, pelvis and clavicle, participant's skin and bones were considered along specific axes. The frontal axis was assumed for the trochanter, while the sagittal axis was used for the pelvis and clavicle. In the spine region, data were modified only based on the markers' dimensions, as skinfold thickness measurements on top of the spinous processes were unavailable. A spline was fitted to connect the locations of the spine markers, with the participant's skin points assumed to be perpendicular to this curve at the corresponding marker's position.

Joints Calculation

An estimation of the human body joints was conducted. For the elbow, wrist, knee, and ankle joints, the joint centres were estimated as the average point between their corresponding lateral and medial markers, as outlined in [17-18]. Regarding the shoulder joint, following the methodology described in [17], the centre was estimated according to [19], where it was assumed to be translated from the shoulder marker in negative vertical direction by a value equal to 17% of the shoulder-to-shoulder distance. The calculation of the hip joint centre followed the approach outlined by [20], also described in [17]. Utilising the trochanter markers, the joint centre was estimated to be translated medially in the trochanter-to-trochanter direction by a value equal to 25% of the trochanter-to-trochanter distance.

Characteristic Angles Calculation

By utilising predefined joint centres and additional anatomical landmarks across various body regions, such as the head, spine, pelvis, hands, and feet, the posture of each bicyclist riding the three bicycles can be visually depicted through a kinematic linkage model, similar to those utilized for occupants [21], for power two and three-wheeler riders [17], for electric scooters [22], and for e-scoters [18]. Figure 2 illustrates a volunteer riding the city bike at a pedal angle of 0°. This visualisation involves a total of 36 interconnected points forming sequential body segments. Each lower extremity is represented by four points, corresponding to the hip (Hi), knee (Kn), ankle (An) joints, and toe (To). Similarly, four points on each upper extremity represent the shoulder (Sh), elbow (El), wrist (Wr) joints, and fingers (Fi). Additionally, five points were positioned on the head, with four of them establishing the Frankfort plane, denoting the upper margin of the opening of external auditory canals (Tr) and the lower margin of the orbits (Ob), and one was positioned on the occipital bone (O). Two points are defined on each scapula (SS, SI) and four additional points on the pelvis represent the PSIS and ASIS points. Finally, seven more points are identified on the spine, depicting the spinous processes of C7, T4, T7, T10, T12, L3, and L5 vertebrae.

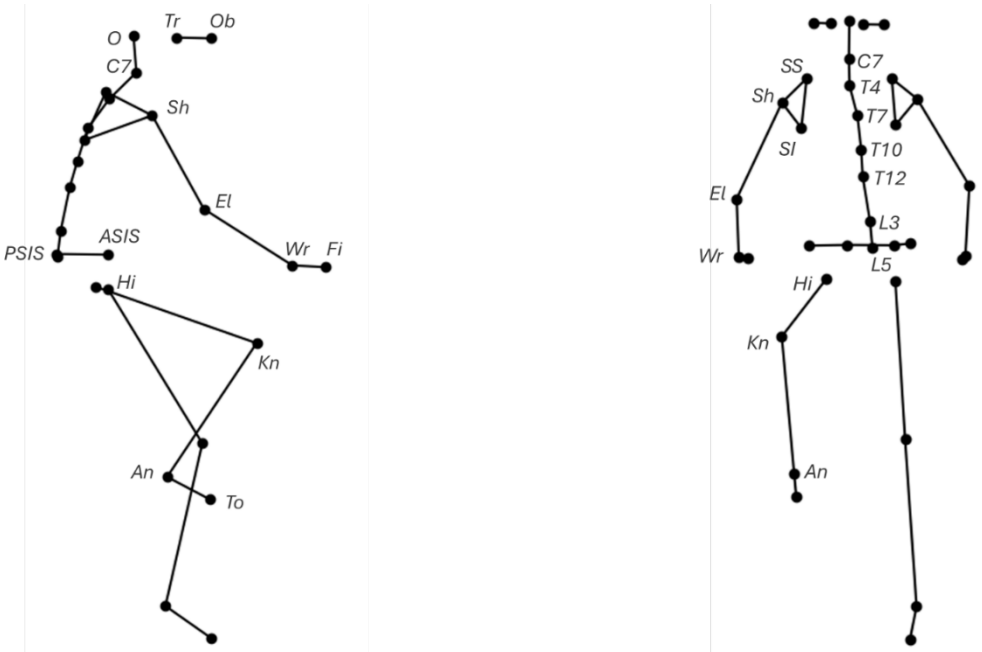

Fig. 2. Kinematic linkage model of a participant riding the city bicycle at a pedal angle of 0°. Participant's joint centres and anatomical points are shown on spine, pelvis, and right upper and lower extremities. The corresponding points exist on the left upper and lower extremities.

Using the segments formed between the joint centres and anatomical landmarks, various characteristic angles of the bicyclist's posture were computed individually for each volunteer riding each bicycle across all analysed pedal angles. These characteristic angles were defined between adjacent segments, and between segments and anatomical planes, similar to those described in [17-18] [21-22]. The equations utilized to calculate the magnitude of each characteristic angle can be found in Table BI of the Appendix. Figures 3–7 present these characteristic angles along with their polarity.

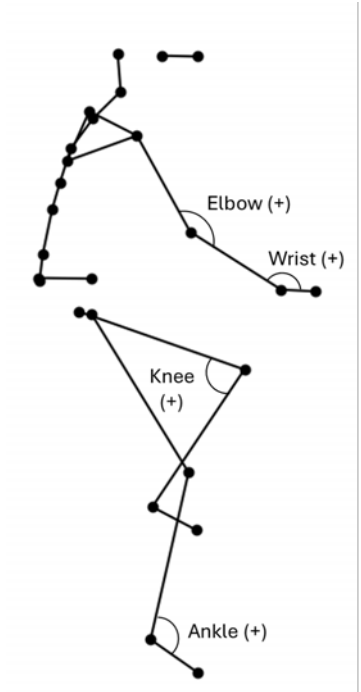

Fig. 3. Characteristic angles formed between segments.

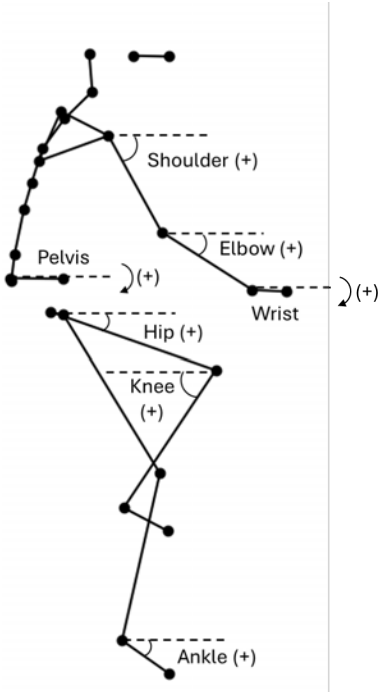

Fig. 4. Characteristic angles of upper and lower extremities and pelvis, formed in the sagittal plane.

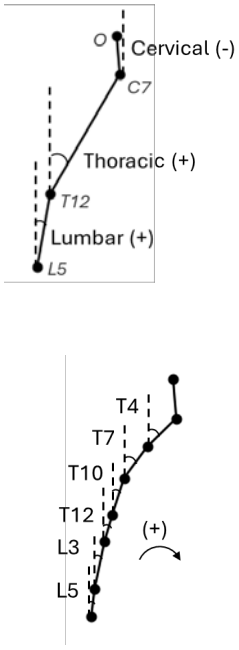

Fig. 5. Characteristic angles of spine segments and vertebrae, formed in the sagittal plane.

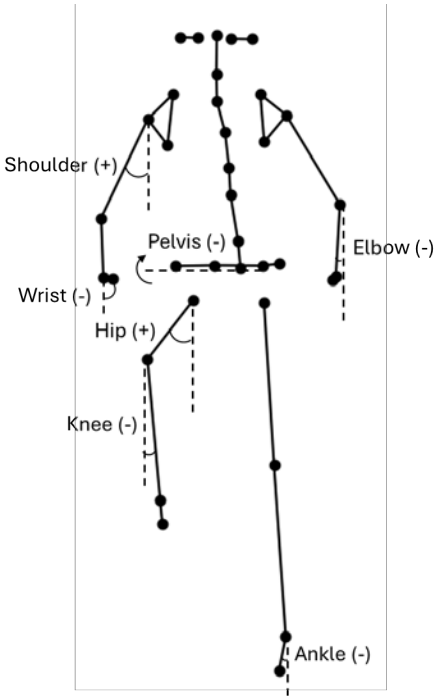

Fig. 6. Characteristic angles of upper and lower extremities and pelvis, formed in the frontal plane.

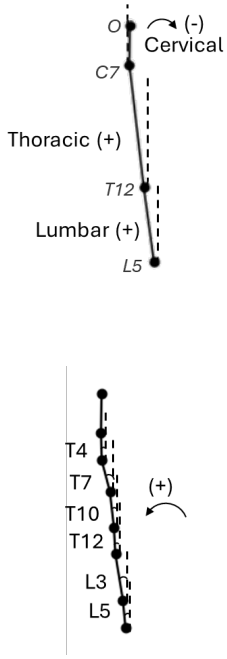

Fig. 7. Characteristic angles of spine segments and vertebrae, formed in the frontal plane.

Average Posture Calculation

Utilising the length of the segments formed between the joint centres and anatomical landmarks, as well as the characteristic angles derived from all participants, the average bicyclist posture for each bicycle and pedal angle could be identified. This process involved calculating the mean and standard deviation of the segment lengths, and the mean and standard deviation of the characteristic angles across all participants for each bike and pedal angle. Subsequently, linkage models similar to those of the participants, representing the calculated average postures, could be created using the mean segment length and mean characteristic angles.

III. RESULTS

Participants' Anatomical Dimensions

A calculation of the mean value and deviation in participants' height and weight is conducted. The participants' mean height is calculated as 176.4 cm with a deviation of 3.2 cm, while the participants' mean weight is calculated as 75.4 kg with a deviation of 3.7 kg.

Participants' Biking Speed

The mean value and standard deviation of participants' biking speed for each bicycle type were calculated. The biking speeds were 115.9 ± 38.9 deg/sec for the city bike, 157.3 ± 66.6 deg/sec for the racing bike, and 136.9 ± 56.9 deg/sec for the mountain bike. Detailed information regarding each participant's biking speed on each bicycle can be found in Table CI of the Appendix.

Participants' Average Posture

Figure 8 illustrates kinematic linkage models generated to represent the average bicyclist posture for each bicycle at a pedal angle of 0°, providing insights into the posture variation among the three bikes. To facilitate comparison, the three linkage models are aligned at the midpoint of the pedals' rotation axis, specifically at the middle of the left and right 'PEc' points, as shown in Fig. A4 of the Appendix. Noticeable differences are observed in the pelvis and upper body of the average posture among the three bikes. The racing bicycle induces a more forward-leaning posture, characterised by a greater flexion in both the lumbar and thoracic spine. Specifically, these angles measure 10°±7° (lumbar angle) and 33°±3° (thoracic angle) in the city bike, 27°±9° and 54°±4° in the mountain bike, and 44°±5° and 73°±3° in the racing bike, respectively. Additionally, a larger pelvis tilt angle is observed in the sagittal plane for the racing bike compared to the city and mountain bikes. Furthermore, the

racing bicycle results in a posture with elbows closer to the torso. Conversely to the upper body, the lower body of the participants exhibits similar characteristics across the three bicycle types. The most notable deviation is observed in the left knee segment angle, ranging from 135°±7° in the city bicycle to 123°±7° in the mountain bike. Further details regarding the mean characteristic angles and the mean segment lengths for the three different bicycle types for each pedal angle are provided in Tables DI to DXV of the Appendix.

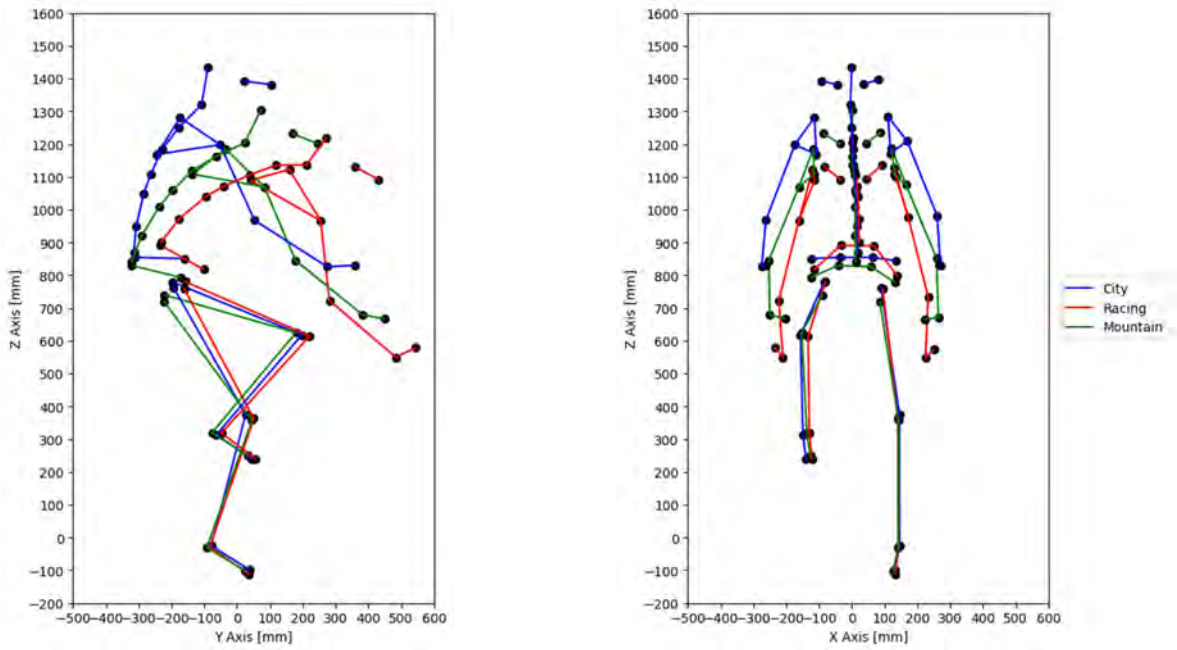

Fig. 8. Kinematic linkage models created from the mean characteristic angles and mean segment lengths of participants riding the city (blue), racing (red), and mountain (green) bikes at pedal angle of 0°.

In Fig. 9, the average bicyclist postures for the city bicycle are depicted for pedal angles ranging from 0° to 180° with 30° increments. Similar to Fig. 8, the linkage models are aligned at the midpoint of the pedals' rotation axis. For clarity, only the posture of the right leg is presented in the sagittal plane. The upper extremities exhibit relatively constant positions through the pedaling in both the frontal and sagittal planes. Minor deviations are observed in the spine's characteristic angles in the sagittal plane, while in the frontal plane the mean lumbar and mean thoracic angles deviate up to 4° and 6° respectively, for pedal angles from 0° to 180°. As anticipated, larger deviations are observed in the lower extremities, where the hip sagittal, knee segment, and ankle segment angles increase throughout the pedaling. Moreover, the right hip angle in the frontal plane decreases, leading to adduction of the right knee as the corresponding leg moves from its upper to its lower position. Conversely, the left leg exhibits the opposite effect, resulting in abduction of the left knee. Similar figures for the racing and the mountain bike can be found in Figures D1-D2 in the Appendix.

Figures 10 to 12 illustrate how the mean characteristic angles, along with their standard deviations, change during pedaling for the three bicycle types. In the figures, the mean characteristic angle is represented by 'x', while the obtained angles of each participant are depicted as 'o'. The X-axis shows the current pedal angle, while the Y-axis represents the characteristic angle. In Fig. 10, the calculated mean characteristic angles with their standard deviations for the right hip joint in the frontal plane, the right knee segment, and the right ankle segment angles are depicted. All angles exhibit similar cycling behaviours for the three bikes through the pedaling, likely due to the consistent motion of the lower extremities. The mean hip joint angle decreases from 0° to 180°, indicating the adduction of the right knee, as previously observed in Fig. 8, while its subsequent increase from 180° to 360° signifies the subsequent abduction of the knee. The standard deviation remains consistent across the three bikes through the pedaling, displaying a decreasing trend until 180° followed by an increasing trend until 360°. The mean knee segment angle exhibits an increasing trend, revealing the extension of the right knee up to the 180° pedal angle, followed by a decreasing trend indicating its flexion. The mean ankle segment angle remains almost constant until 90°, when the foot moves from its upper to the most frontal position, followed by an increasing trend as it descents to its lower position. Finally, while returning to its upper position, the angle shows a decreasing trend. In both the knee segment and ankle segment angles, all bikes exhibit similar standard deviation of the mean angles.

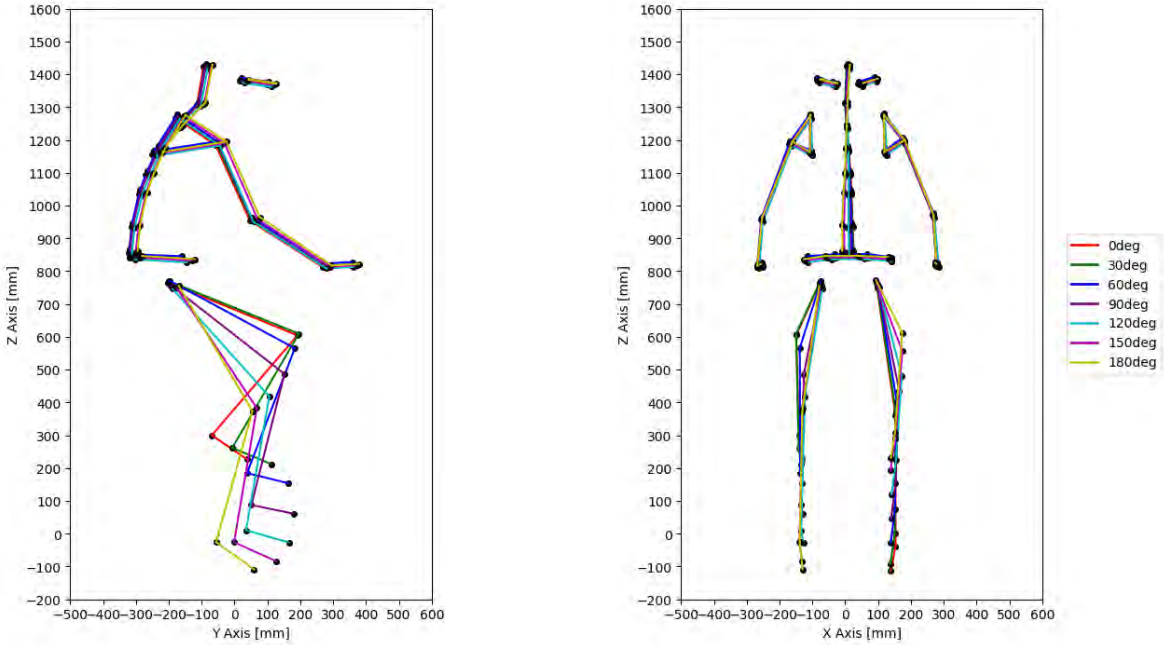

Fig. 9. Kinematic linkage models created from the mean characteristic angles and mean segment lengths of participants riding the city bike at pedal angles from 0° to 180°, with 30° increments.

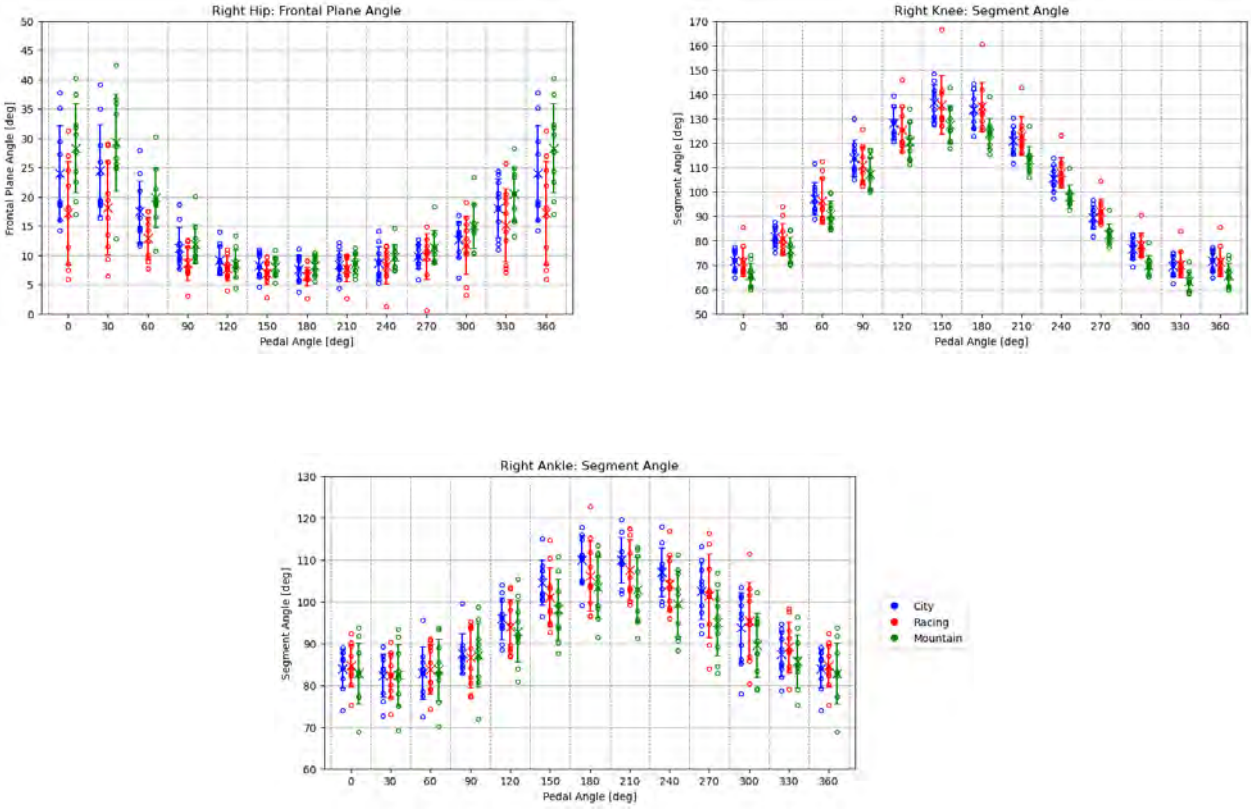

Fig. 10. Mean right hip angle in frontal plane (upper left), mean right knee segment angle (upper right), mean right ankle segment angle (lower), for city, racing, and mountain bikes at each pedal angle.

In Fig. 11, the mean characteristic angles along with their standard deviations for the right shoulder in the frontal and sagittal planes, and the right elbow and right wrist segment angles are depicted for each bike. All mean characteristic angles along with their standard deviations, remain almost constant throughout pedaling for each bike. However, noticeable differences in the mean angles across the bikes are observed. The mean characteristic angles of the shoulder, in both frontal and sagittal planes, and of the elbow, exhibit great

differences for the racing bike compared to the city and mountain bikes, indicating a more flexed elbow position closer to the torso. The wrist segment angle shows the greatest deviation between bikes, with the racing bike differing more due to its different handlebar geometry, leading to an altered handlebar grip.

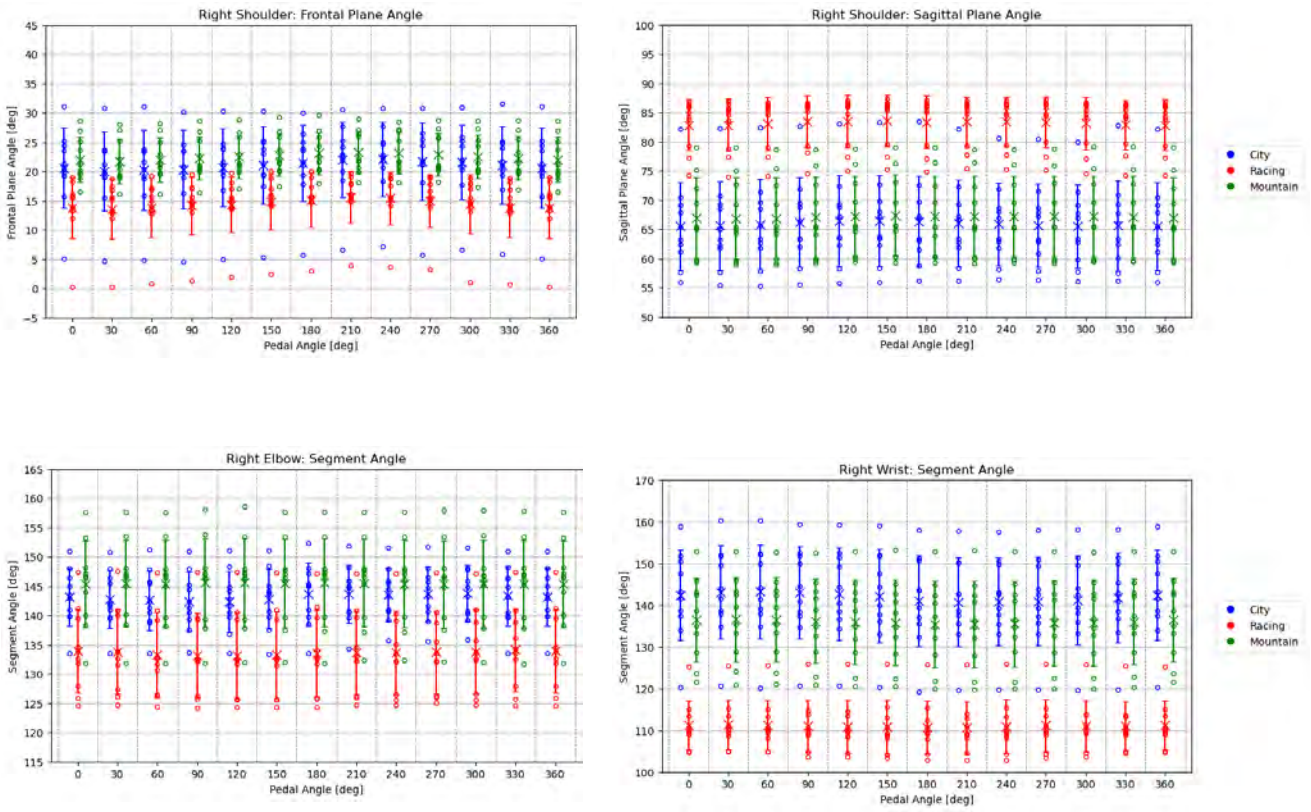

Fig. 11. Mean right shoulder angle in frontal plane (upper left) right shoulder angle in sagittal plane (upper right), mean right elbow segment angle (lower left), mean right wrist segment angle (lower right), for city, racing, and mountain bikes at each pedal angle.

Figure 12 illustrates the movement of the pelvis and the thoracic and lumbar spine in the frontal plane. Similar to Figure 10, the mean characteristic angles demonstrate a consistent cycling pattern across all three bikes. However, notable differences are observed between the movement of the pelvis and the spine. While both the lumbar and thoracic spine regions lean towards the right when the right pedal is at its upper position (pedal angle of 0°), almost aligning with the Z-axis when the legs are parallel to the horizontal plane at 90° and 270° pedal angles, and lean left when the left leg moves upwards, the pelvis exhibits movement in the opposite direction. It leans to the left at 0°, rotates to the right until reaching 180°, and then rotates to the left again. Moreover, the thoracic segment's lean is notably larger than that of the pelvis and lumbar spine for all three bikes. The racing bicycle shows the largest deviations in mean characteristic angles through the pedaling, with values equal to 6° for the pelvis, 5° for the lumbar spine, and 16° for the thoracic segment. The standard deviations of the mean lumbar and pelvis angles exhibit similar values across the three bikes, while a greater standard deviation of the mean thoracic angle is observed for the racing bike, indicating a wider range of right and left lean among participants. Further figures illustrating the deviation of mean characteristic angles at each pedal angle are provided in Figures D3 to D11 in the Appendix.

To facilitate the comparison of characteristic angles demonstrating cycling patterns through pedaling among the three bikes, particularly for the spine and pelvis frontal plane angles, as well as lower extremities segment, frontal plane, and sagittal plane angles, sine waves were fitted to the calculated mean values. Their coefficients can be found in Table DXVI of the Appendix.

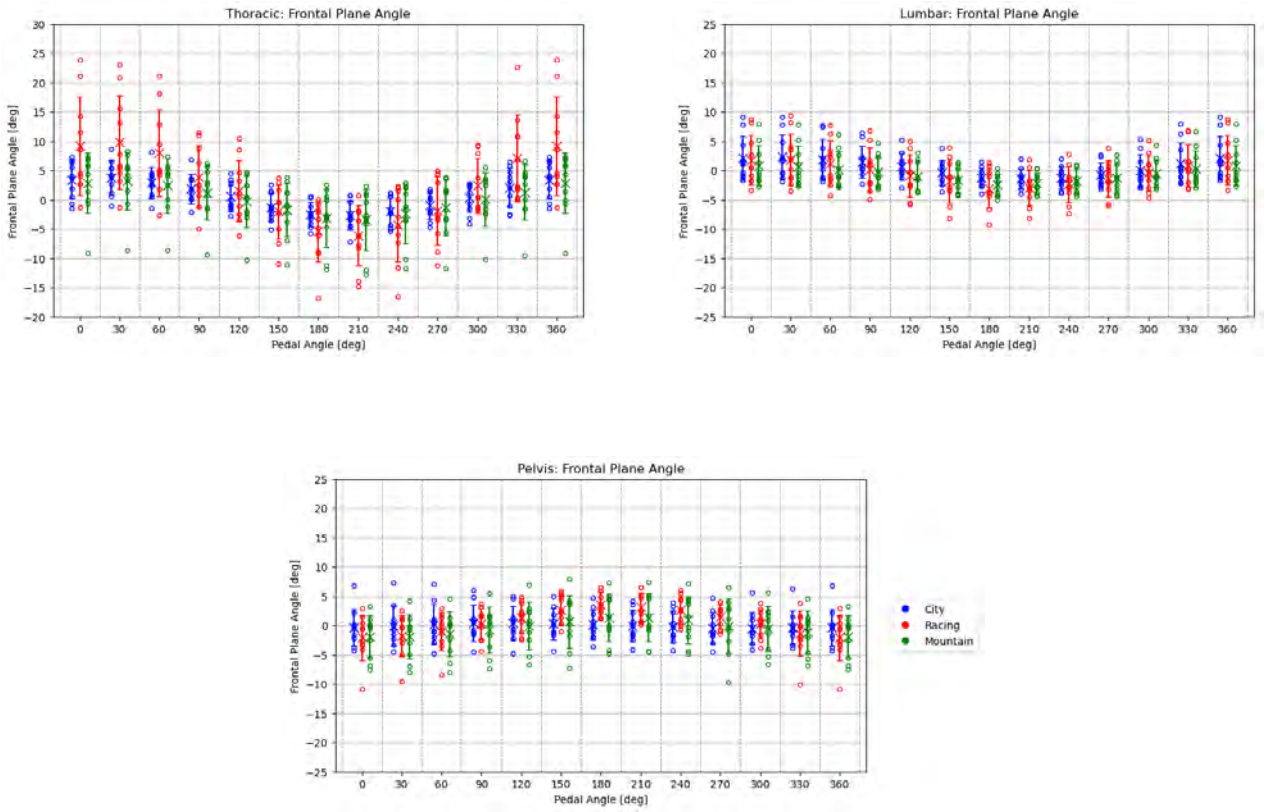

Fig. 12. Mean thoracic (upper left), lumbar (upper right), pelvis (lower) angle in frontal plane for city, racing, and mountain bikes at each pedal angle.

IV. DISCUSSION

Overall, the study collected and analysed the postures of 10 male volunteers (50th percentile) through photogrammetric measurements of 52 anatomical landmarks while riding three different types of bike: city, racing, and mountain. The average bicyclist posture was determined through the calculation of participants' characteristic angles, for each bike and for pedal angles ranging from 0° to 360°, with 30° increments, allowing the examination of posture variations throughout the pedaling and across different bicycle types.

The pedal angle during a bicycle crash is crucial for determining bicyclist's injuries and impact kinematics. Research indicates that the pedal's position significantly affects injury outcomes. For instance, [4] shows that in bicycle-vehicle collisions, higher brain strain values occur when the impacted leg is in its most forward position, while higher neck ligament tension is observed with the impacted leg in its upper position. Additionally, [10] indicates that pedal angle influences the head impact angle and primary impact location, altering the loading of the impacted leg. Therefore, this study calculated the average bicyclist posture for various pedal angles to enable the examination of how pedal angle variations may impact bicyclist kinematics and injuries in several crash scenarios.

The results of the study showed that the mean height calculated across participants exhibited a deviation of 1.4 cm from the corresponding value of the average male specified in [14], representing a deviation of 0.8%. Similarly, the mean weight exhibited a 2% deviation compared to the average value in [14]. However, greater emphasis was placed on height criteria during participant selection, due to its presumed greater importance in accurately positioning HBMs. A larger deviation in height may complicate the precise alignment of the HBM to fit the bicycle's saddle while ensuring its ability to reach both the pedals and handlebar simultaneously.

The study's findings revealed variability in average biking speeds, particularly notable for the racing bike. While participants were instructed to maintain a slow biking speed, no specific speed was prescribed. This lack of standardization in biking speed may have contributed to the observed deviations in posture among participants. It is important to acknowledge that participants' biking speed can influence their obtained postures. For instance,

higher biking speed may lead to increased torso movement compared to slower speeds. Future research should explore how different biking speeds affect posture, and thereby safety considerations.

Analysis of the mean characteristic angles revealed notable differences in torso movements within the frontal plane, particularly in spine and pelvis motions, exhibiting opposing left- and right-leaning directions throughout pedaling. Specifically, findings suggested a decreasing motion in the frontal plane from the lower thoracic (T12) to the lower lumbar (L5) vertebra for all bikes, as depicted in Fig. D6 of the Appendix. This follows a coherent line of reasoning, as the lean appears to decrease when getting lower in the spine before the opposite pelvis movement occurs. Moreover, the results suggested the nearly constant lower extremities position in the frontal plane and its significant variation in the sagittal plane, where hip, knee, and ankle flexion and extension were distinctly visible throughout the pedaling cycle. Results indicated that no significant spine flexion or extension, or pelvis tilt modification, occurred during biking. Moreover, mean characteristic angles of the upper extremities remained relatively stable throughout the pedaling motion, with no apparent abduction, adduction, flexion, or extension.

Regarding the differences in mean characteristic angles between the bikes, greater deviations were noted in the upper body than in the lower body. This can be attributed to the greater variation in the saddle-to-handlebar geometry (SAb-to-HBb) compared to the saddle-to-pedal geometry (SAb-to-PEc) between the bikes. The slight deviation of lower extremities angles between the bikes may also be influenced by the bike fitting process, which restricts their reachable angle values. In this context, the spine and pelvis exhibited the most variability between the city and racing bikes. Specifically, the deviation in the mean characteristic angles in the sagittal plane between city and racing bikes, averaged 30° for the pelvis, 35° for the lumbar spine, and 39° for the thoracic spine during the pedal cycle.

Results suggested that the most notable differences in mean characteristic angles of upper extremities were observed in the wrist joint. These differences averaged 31° for the segment angle, 116° in the frontal plane angle, and 31° in the sagittal plane angle, considering both left and right sides across all pedal angles. The variations arise from the distinct handlebar shapes of the three bike types. The mountain bike features a nearly straight handlebar, lacking significant bending between its left and right sides. The city bike features a handlebar with a triangular shape, resulting in a distinctive grip. The racing bicycle's handlebar is shaped like a rotated 'U', allowing for various grips. However, when braking in racing bike, as instructed for volunteers, the rider's palms must face each other, unlike the other two bikes where the palms align in the same direction. As a result, the distinct handlebar designs necessitated different wrist angles between the bikes.

As discussed, differences in the mean characteristic angles of lower extremities across the bikes are comparatively smaller. However, the standard deviations observed for each bike likely arise from variations in feet placement on the pedals, as volunteers obtained their preferred feet position.

In general, the average bicyclist posture calculated for the racing bike appears the most distinct compared to the other two bikes. This can be attributed to its lower vertical saddle-to-handlebar distance, which on average for all participants is about 84% lower than that of the city bike and 72% lower than that of the mountain bike, alongside its unique handlebar geometry. These factors significantly influence the rider's posture, promoting a more aerodynamic position characterised by a higher pelvis tilt angle, increased flexion in the thoracic and lumbar spine, and a closer positioning of the upper extremities to the torso.

While this study provides valuable insights into the average bicyclist's posture, it is subjected to several limitations. First, the small sample size of 10 participants restricts the generalisability of the results, underscoring the necessity for larger testing groups to improve result reliability. Additionally, while the three analysed bikes (city, racing, mountain) were selected for their distinct saddle-handlebar-pedal distances, they only provide insights into the posture obtained for these specific bikes. To obtain more generalised results representative of the entire bicyclist population, further examination of bicyclist posture across a broader range of bicycle types is necessary.

Moreover, the bike fitting process was conducted based on general guidelines rather than a specific method tailored to each individual bike type. A more appropriate method, ideal for the measured bike type, may lead to the selection of a different bike saddle height, and thereby to different obtained postures.

In addition, the study focused only on understanding the posture of the 50th percentile male, resulting in participant selection aimed at minimising variation in height and weight. While this approach reduces sample variability, it limits the generalisability of the findings to the broader bicyclist population. Further research

involving participants with diverse characteristics, including individuals of different genders, ages, heights, weights, and ethnic backgrounds, is necessary to comprehensively understand bicyclist posture across various demographic groups.

Although radiographic images were not used due to ethical concerns, photogrammetric techniques were adopted. However, this method introduces uncertainties. Landmark identification through palpation may lead to errors, and movement between the skin and bones can cause marker displacement. Additional processing of data was necessary to represent the bony structure accurately, involving subtracting marker dimensions and skinfold thickness. To minimise errors, consistent palpation and marker repositioning were performed by experienced operators.

Another limitation of the study is the lack of calculation of vertebral joint centres due to the absence of an established methodology for estimating vertebral centres. As a result, while most joint centres were represented through their estimated points, the vertebral spinous processes were utilised for the spine region, and the characteristic angles of the spine were calculated based on them.

The identified average bicyclist postures are crucial for positioning HBMs and enabling their application in crash simulations, thereby providing valuable insights into bicyclists' injuries and factors influencing accidents, potentially leading to the identification of strategic measures aimed at mitigating such incidents. Previous studies often positioned bicyclists in simulations based on a posture that simply fits the bike rather than using experimental data. By utilising the calculated mean segment lengths and the mean characteristic angles across participants for each pedal angle and bike, the average posture can be produced and implemented in HBMs for running crash simulations. The crash simulation results can be used to optimise bicyclist safety equipment, such as helmets and protective scarves [4][13], and to redesign vehicle attributes, as well as enhance cycling infrastructure and urban planning.

V. CONCLUSION

In this study, postures' definition was derived from 3D photogrammetric measurements of anatomical landmarks on 10 participants while riding three types of bicycle: city, racing, and mountain. The post-processing of the measurements enabled the determination of the average bicyclist posture of the 50^{th} percentile male for each bike type. The bicyclist posture was determined for multiple bike pedal angles, ranging from 0° to 360°, with 30° increments. The posture analysis revealed that the segment characteristic angles of the lower extremities were the most influenced by pedaling for all bikes. Upper extremities exhibited almost constant characteristic angles, while leaning of the pelvis and spine was observed in the characteristic angles of the frontal plane. Additionally, the study highlighted that the differences between bikes are more significant in the pelvis, spine region, and upper extremities.

The identified bicyclist postures can be applied to the Human Body Models to conduct crash simulations and to provide information on bicyclists' kinematics and injuries during crash. These investigations can be used to enhance the bicyclists' safety systems and improve the urban infrastructure.

VI. ACKNOWLEDGEMENTS

The study was financed by BETA CAE Systems SA.

VII. REFERENCES

[1] European Commission (2022) Road Safety Thematic Report – Cyclists. European Road Safety Observatory. Brussels, European Commission, Directorate General for Transport.

[2] Dash, I., Abkowitz, M., Philip, C. (2022) Factors impacting bike crash severity in urban areas. *Journal of Safety Research*, **83**: pp. 128–138.

[3] Bahrololoom, S., Young, W., Logan, D. (2020) Modelling injury severity of bicyclists in bicycle-car crashes at intersections. *Accident Analysis & Prevention*, **144**: p.105597.

[4] Alvarez, V., Malalla, A., *et al*. (2022) Predicting Head and Neck Injury in Bicycle Accident Simulations. *Proceedings of Human Modeling and Simulation in Automotive Engineering*, 2022, Wiesbaden, Germany.

[5] Peng, Y., Chen, Y., Yang, J., Otte, D., Willinger, R. (2012) A study of pedestrian and bicyclist exposure to head injury in passenger car collisions based on accident data and simulations. *Safety Science*, **50**(9): pp. 1749–1759.

[6] Maki, T. and Kajzer, J. (2001) The behavior of bicyclists in frontal and rear crash accidents with cars. *JSAE Review*, **22**(3): pp. 357–363.
[7] Katsuhara, T., Miyazaki, H., Kitagawa, Y., Yasuki, T. (2014) Impact Kinematics of Cyclist and Head Injury Mechanism in Car-to-Bicycle Collision. *Proceedings of the IRCOBI Conference*, 2014, Berlin, Germany.
[8] Monfort, S. S. and Mueller, B. C. (2023) Bicyclist crashes with cars and SUVs: Injury severity and risk factors. *Traffic Injury Prevention*, **24**(7): pp. 645–651.
[9] Huang, Y., Zhou, Q., Koelper, C., Li, Q., Nie, B. (2020) Are riders of electric two-wheelers safer than bicyclists in collisions with motor vehicles? *Accident Analysis & Prevention*, **134**: p.105336.
[10] Zander, O. and Hamacher, M. (2017) Revision of passive pedestrian test and assessment procedures to implement head protection of cyclists. *Proceedings of the 25th International Technical Conference on the Enhanced Safety of Vehicles (ESV)*, 2017, Detroit, Michigan, USA.
[11] Pal, C., Vallabhaneni, P., Kulothungan, V., Manoharan, J., Shigeru, H. (2021) AF05 Bicyclist's Head Kinematics in Car-to-Ebike Perpendicular and Angular Impacts. *International Journal of Automotive Engineering*, **12**(1): pp. 16–23.
[12] Pal, C., Hirayama, S., Vallabhaneni, P., Vimalathithan, K., Manoharan, J. (2020) Comparison of Head Kinematics of Bicyclist in Car-to-Bicycle Impact. SAE Technical Paper (Paper number: 2020-01-0932).
[13] Alvarez, V., Wendelrup, H., Brolin, K. (2021) Analyzing bicycle accidents with human body models. *Proceedings of the 13th European LS-DYNA Conference*, 2021, Ulm, Germany, pp. 134–135.
[14] Schneider, L. W., Robbins, D. H., Pflug, M. A., Snyder, R. G. (1983) Development of anthropometrically based design specifications for an advanced adult anthropomorphic dummy family. University of Michigan Transportation Research Institute, Ann Arbor, Michigan, USA.
[15] Wu, G., Siegler, S., et al. (2002) ISB recommendation on definitions of joint coordinate system of various joints for the reporting of human joint motion--part I: ankle, hip, and spine. *Journal of Biomechanics*, **35**: pp. 543–548.
[16] Wu, G., van der Helm, F.C., et al. (2005) ISB recommendation on definitions of joint coordinate systems of various joints for the reporting of human joint motion--Part II: shoulder, elbow, wrist and hand. *Journal of Biomechanics*, **38**: pp. 981–992.
[17] Lundin, L., Oikonomou, M., et al. (in press) Quantifying Rider Posture Variability in Powered Two- and Three-Wheelers for Safety Assessment. *Traffic Injury Prevention.*
[18] Leo, C., Schachner, M., Kofler, D., Klug, C. (2023) E-scooter Driving Postures and Velocities Retrieved from Volunteer Tests using Motion Capturing and Traffic Observations. *Proceedings of the IRCOBI Conference*, 2023, Cambridge, UK.
[19] Rab, G., Petuskey, K., Bagley, A. (2002) A method for determination of upper extremity kinematics. *Gait & Posture*, **15**(2): pp. 113–119.
[20] Weinhandl, J. T. and O'Connor, K. M. (2010) Assessment of a greater trochanter-based method of locating the hip joint center. *Journal of Biomechanics*, **43**(13): pp. 2633–2636.
[21] Reed, M.P., Manary, M.A., Flannagan, C.A., Schneider, L.W. (2002) A statistical method for predicting automobile driving posture. Human Factors, **44(**4): 557-568.
[22] Chou, J.R. and Hsiao, S.W. (2005) An anthropometric measurement for developing an electric scooter. *International Journal of Industrial Ergonomics*, **35**: pp.1047-1063.

VIII. APPENDIX

A. Experimental Data Collection

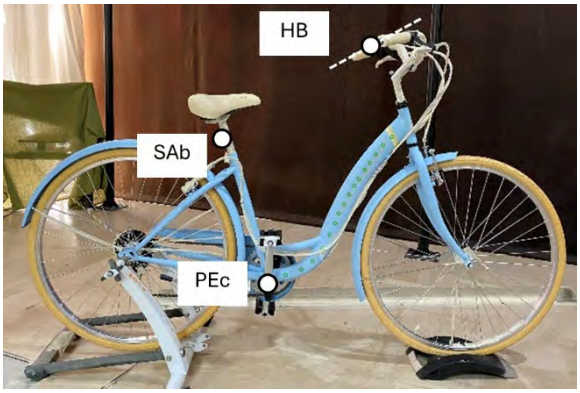

Fig. A1. City bicycle showing the saddle's base point (SAb), the handlebar's middle point (HB), and the pedals' rotation axis point (PEc).

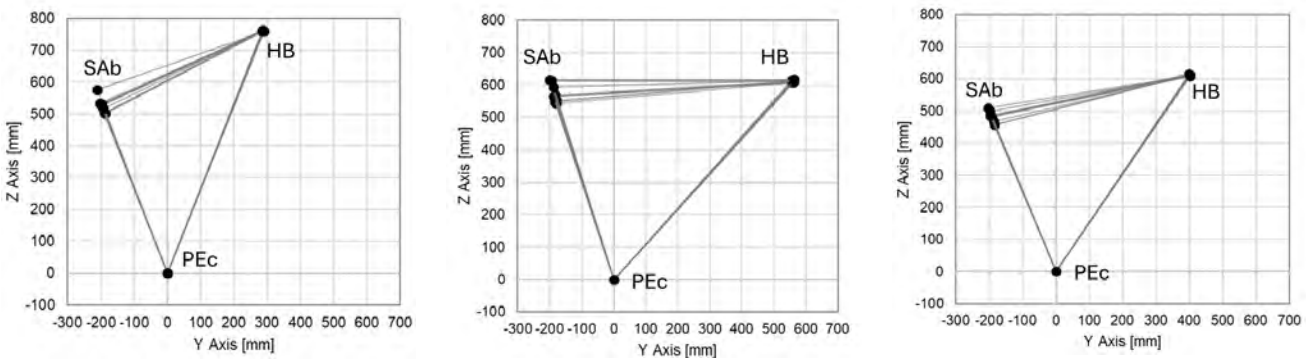

Fig. A2. Geometric triangles of the city (left), racing (middle), and mountain (right) bikes, formed for each participant between the saddle's base point (SAb), the handlebar's middle point (HB), and the pedals' rotation axis point (PEc).

Fig. A3. Participant with reflective markers placed on his anatomical landmarks. Front view (left), side view (middle), and back view (right).

TABLE AI
REFLECTIVE MARKERS' DESCRIPTION

Body Segment	Name	Number	Location	Description
Head	Ob	2	left & right side	Inferior margin of the orbit
	Tr	2	left & right side	Tragus
	Occ	2	left & right side	Articular process behind the ear
	O	1	central	Occiput
Arms	Gh	2	left & right side	Most dorsal point on the acromioclavicular joint, shared with the scapula
	Le	2	left & right side	Most caudal point on lateral epicondyle
	Me	2	left & right side	Most caudal point on medial epicondyle
	Rs	2	left & right side	Most caudal-lateral point on the radial styloid
	Us	2	left & right side	Most caudal-medial point on the ulnar styloid
	Fi	2	left & right side	Head of the 2nd metacarpal
	Fi5	2	left & right side	Head of the 5th metacarpal
Scapula	SS	2	left & right side	Spine of scapula
	SI	2	left & right side	Inferior angle of scapula
Clavicle	CLV	2	left & right side	External extremity of clavicle
Pelvis	ASIS	2	left & right side	Anterior superior iliac spine
	PSIS	2	left & right side	Posterior superior iliac spine
Legs	T	2	left & right side	Trochanter
	Lc	2	left & right side	The most lateral point on the border of the femoral condyle
	Mc	2	left & right side	The most medial point on the border of the medial femoral condyle
	Lm	2	left & right side	Tip of the lateral malleolus
	Mm	2	left & right side	Tip of the medial malleolus
	To	2	left & right side	Head of the 1st metatarsal
	Hl	2	left & right side	Most rear point of calcaneus
Spine	C7	1	central	Spinous process of the seventh cervical vertebra
	T4	1	central	Spinous process of the fourth thoracic vertebra
	T7	1	central	Spinous process of the seventh thoracic vertebra
	T10	1	central	Spinous process of the tenth thoracic vertebra
	T12	1	central	Spinous process of the twelfth thoracic vertebra
	L3	1	central	Spinous process of the third lumber vertebra
	L5	1	central	Spinous process of the fifth lumber vertebra

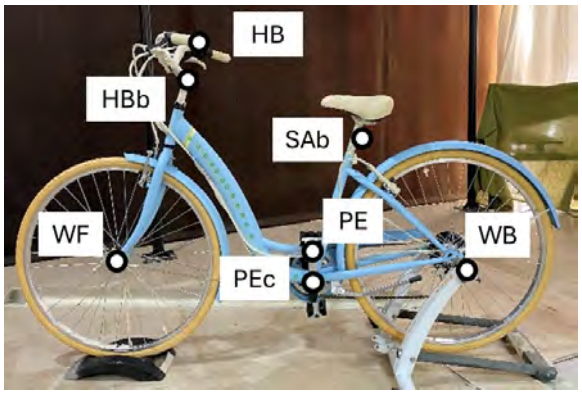

Fig. A4. City bicycle equipped with the reflective markers. Markers are placed on the left and right side of forward (WF) and backward wheels (WB), on the left and right side of pedals' rotation axis (PEc), on the left and right pedals (PE), on saddle's base (SAb), on handlebar's base (HBb), and on the left and right handlebar's ends (HB).

B. Characteristic Angles Calculation

TABLE BI
EQUATIONS TO CALCULATE CHARACTERISTIC ANGLES' MAGNITUDE

	Angle	Segment 1	Segment 2	Equation
Segment to Segment	Elbow	Sh-El	El-Wr	$\cos^{-1}\left(\left(\overrightarrow{Sh\ El}\cdot\overrightarrow{El\ Wr}\right)/\left(\left\|\overrightarrow{Sh\ El}\right\|*\left\|\overrightarrow{El\ Wr}\right\|\right)\right)$
	Wrist	El-Wr	Wr-Fi	$\cos^{-1}\left(\left(\overrightarrow{El\ Wr}\cdot\overrightarrow{Wr\ Fi}\right)/\left(\left\|\overrightarrow{El\ Wr}\right\|*\left\|\overrightarrow{Wr\ Fi}\right\|\right)\right)$
	Knee	Hi-Kn	Kn-An	$\cos^{-1}\left(\left(\overrightarrow{Hi\ Kn}\cdot\overrightarrow{Kn\ An}\right)/\left(\left\|\overrightarrow{Hi\ Kn}\right\|*\left\|\overrightarrow{Kn\ An}\right\|\right)\right)$
	Ankle	Kn-An	An-To	$\cos^{-1}\left(\left(\overrightarrow{Kn\ An}\cdot\overrightarrow{An\ To}\right)/\left(\left\|\overrightarrow{Kn\ An}\right\|*\left\|\overrightarrow{An\ To}\right\|\right)\right)$
Frontal Plane	Shoulder	Sh-El	-	$\tan^{-1}((El_x - Sh_x)/(El_z - Sh_z))$
	Elbow	El-Wr	-	$\tan^{-1}((Wr_x - El_x)/(Wr_z - El_z))$
	Wrist	Wr-Fi	-	$\tan^{-1}((Fi_x - Wr_x)/(Fi_z - Wr_z))$
	Hip	Hi-Kn	-	$\tan^{-1}((Kn_x - Hi_x)/(Kn_z - Hi_z))$
	Knee	Kn-An	-	$\tan^{-1}((An_x - Kn_x)/(An_z - Kn_z))$
	Ankle	An-To	-	$\tan^{-1}((To_x - An_x)/(To_z - An_z))$
	T4	T4-C7	-	$\tan^{-1}((C7_x - T4_x)/(C7_z - T4_z))$
	T7	T7-T4	-	$\tan^{-1}((T4_x - T7_x)/(T4_z - T7_z))$
	T10	T10-T7	-	$\tan^{-1}((T7_x - T10_x)/(T7_z - T10r_z))$
	T12	T12-10	-	$\tan^{-1}((T10_x - T12_x)/(T10_z - T12_z))$
	L3	L3-T12	-	$\tan^{-1}((T12_x - L3_x)/(T12_z - L3_z))$
	L5	L5-L3	-	$\tan^{-1}((L3_x - L5_x)/(L3_z - L5_z))$
	Cervical	C7-O	-	$\tan^{-1}((O_x - C7_x)/(O_z - C7_z))$
	Thoracic	T12-C7	-	$\tan^{-1}((C7_x - T12_x)/(C7_z - T12_z))$
	Lumbar	L5-T12	-	$\tan^{-1}((T12_x - L5_x)/(T12_z - L5_z))$
	Pelvis	PSISl-PSISr	-	$\tan^{-1}((PSISr_z - PSISl_z)/(PSISr_x - PSISl_x))$
Sagittal Plane	Shoulder	Sh-El	-	$\tan^{-1}\left((El_z - Sh_z)/\left(El_y - Sh_y\right)\right)$
	Elbow	El-Wr	-	$\tan^{-1}\left((Wr_z - El_z)/\left(Wr_y - El_y\right)\right)$
	Wrist	Wr-Fi	-	$\tan^{-1}\left((Fi_z - Wr_z)/\left(Fi_y - Wr_y\right)\right)$
	Hip	Hi-Kn	-	$\tan^{-1}\left((Kn_z - Hi_z)/\left(Kn_y - Hi_y\right)\right)$
	Knee	Kn-An	-	$\tan^{-1}\left((An_z - Kn_z)/\left(An_y - Kn_y\right)\right)$
	Ankle	An-To	-	$\tan^{-1}\left((To_z - An_z)/\left(To_y - An_y\right)\right)$
	T4	T4-C7	-	$\tan^{-1}\left(\left(C7_y - T4_y\right)/(C7_z - T4_z)\right)$
	T7	T7-T4	-	$\tan^{-1}\left(\left(T4_y - T7_y\right)/(T4_z - T7_z)\right)$
	T10	T10-T7	-	$\tan^{-1}\left(\left(T7_y - T10_y\right)/(T7_z - T10r_z)\right)$
	T12	T12-10	-	$\tan^{-1}\left(\left(T10_y - T12_y\right)/(T10_z - T12_z)\right)$
	L3	L3-T12	-	$\tan^{-1}\left(\left(T12_y - L3_y\right)/(T12_z - L3_z)\right)$
	L5	L5-L3	-	$\tan^{-1}\left(\left(L3_y - L5_y\right)/(L3_z - L5_z)\right)$
	Cervical	C7-O	-	$\tan^{-1}\left(\left(O_y - C7_y\right)/(O_z - C7_z)\right)$
	Thoracic	T12-C7	-	$\tan^{-1}\left(\left(C7_y - T12_y\right)/(C7_z - T12_z)\right)$
	Lumbar	L5-T12	-	$\tan^{-1}\left(\left(T12_y - L5_y\right)/(T12_z - L5_z)\right)$
	Pelvis	PSISl-ASISl	-	$\tan^{-1}\left((ASISl_z - PSISl_z)/\left(ASISl_y - PSISl_y\right)\right)$

C. Participants' biking speed for City, Racing, and Mountain Bikes

TABLE CI

PARTICIPANTS BIKING SPEED FOR CITY, RACING, AND MOUNTAIN BIKES IN DEGREES PER SECOND [DEG/SEC]

	City	Racing	Mountain
Participant 1	97.2	157.3	128.4
Participant 2	120.1	247.1	229.8
Participant 3	122.1	95.0	118.4
Participant 4	76.1	110.6	75.5
Participant 5	162.1	218.7	201.0
Participant 6	169.2	239.5	146.9
Participant 7	138.9	177.4	167.1
Participant 8	143.2	181.7	170.3
Participant 9	54.6	73.1	61.6
Participant 10	75.8	72.7	70.3
Mean	115.9	157.3	136.9
SD	38.9	66.6	56.9

D. Participants' Average Posture

TABLE DI
MEAN CHARACTERISTIC ANGLES AND STANDARD DEVIATION OF UPPER EXTREMITIES FOR CITY BIKR AT EACH PEDAL ANGLE IN DEGREES

Pedal Angle [deg.]		0	30	60	90	120	150	180	210	240	270	300	330
Shoulder Right	Front.	20.6 ± 6.8	20.1 ± 6.8	20.3 ± 6.8	20.3 ± 6.7	20.7 ± 6.6	21.0 ± 6.6	21.5 ± 6.5	22.0 ± 6.4	22.1 ± 6.3	21.7 ± 6.6	21.6 ± 6.4	21.1 ± 6.7
	Sag.	65.6 ± 7.5	65.6 ± 7.6	65.9 ± 7.7	66.2 ± 7.7	66.4 ± 7.8	66.5 ± 7.8	66.3 ± 7.8	66.0 ± 7.5	65.9 ± 7.1	65.7 ± 7.1	65.5 ± 7.1	65.6 ± 7.8
Shoulder Left	Front.	21.6 ± 6.0	22.1 ± 6.2	22.1 ± 6.0	22.1 ± 6.1	21.8 ± 6.0	21.3 ± 6.0	20.8 ± 5.8	20.9 ± 6.7	20.9 ± 6.7	20.7 ± 6.7	21.1 ± 6.5	21.3 ± 6.2
	Sag.	65.2 ± 5.5	65.2 ± 5.4	65.2 ± 5.3	65.1 ± 5.3	64.8 ± 5.4	64.6 ± 5.6	64.6 ± 5.6	64.7 ± 5.4	64.7 ± 5.1	64.5 ± 5.3	64.7 ± 5.1	65.1 ± 5.5
Elbow Right	Front.	5.3 ± 5.4	4.8 ± 5.6	4.4 ± 5.2	4.1 ± 4.6	4.3 ± 4.3	4.8 ± 3.7	5.7 ± 3.5	6.1 ± 3.8	6.0 ± 4.0	6.6 ± 4.8	6.3 ± 4.6	5.8 ± 4.8
	Sag.	32.6 ± 5.5	32.2 ± 5.6	32.3 ± 5.8	32.4 ± 5.8	32.7 ± 5.9	33.3 ± 5.9	33.9 ± 5.9	33.9 ± 5.6	33.6 ± 5.6	33.5 ± 5.6	33.3 ± 5.7	33.0 ± 5.6
	Segm.	143.1 ± 4.9	142.8 ± 5.0	142.6 ± 5.1	142.3 ± 5.1	142.3 ± 5.2	142.8 ± 5.1	143.6 ± 5.4	143.7 ± 5.0	143.5 ± 4.6	143.7 ± 4.7	143.7 ± 4.8	143.4 ± 5.1
Elbow Left	Front.	4.3 ± 3.9	5.0 ± 4.7	5.2 ± 5.2	5.6 ± 5.1	5.5 ± 5.6	5.2 ± 5.7	4.2 ± 6.0	3.0 ± 7.4	3.1 ± 7.1	3.2 ± 5.8	3.4 ± 4.8	3.8 ± 4.4
	Sag.	34.9 ± 8.3	35.1 ± 8.1	35.0 ± 8.0	35.2 ± 8.1	35.0 ± 8.1	34.7 ± 8.0	34.1 ± 7.9	33.8 ± 7.9	33.8 ± 8.0	34.0 ± 8.0	34.1 ± 8.2	34.6 ± 8.3
	Segm.	144.3 ± 5.1	144.3 ± 4.7	144.1 ± 4.4	144.6 ± 4.7	144.7 ± 4.5	144.7 ± 4.3	144.2 ± 4.5	143.3 ± 5.8	143.3 ± 5.8	143.9 ± 5.4	143.9 ± 5.3	144.0 ± 5.2
Wrist Right	Front.	-51.9 ± 26.9	-51.8 ± 26.0	-52.9 ± 24.5	-54.6 ± 22.6	-54.7 ± 22.0	-53.5 ± 22.4	-54.1 ± 23.1	-53.8 ± 23.7	-54.3 ± 24.5	-52.4 ± 27.0	-52.0 ± 27.9	-52.6 ± 27.1
	Sag.	-3.4 ± 5.8	-3.1 ± 5.9	-3.0 ± 5.9	-3.0 ± 5.8	-3.0 ± 5.8	-3.0 ± 5.8	-3.3 ± 5.7	-3.5 ± 5.5	-3.7 ± 5.4	-3.7 ± 5.5	-3.7 ± 5.6	-3.6 ± 5.7
	Segm.	142.4 ± 10.8	143.1 ± 11.1	143.2 ± 11.3	143.0 ± 11.1	142.7 ± 11.1	142.2 ± 11.2	141.1 ± 11.0	140.8 ± 10.6	140.9 ± 10.6	140.9 ± 10.7	141.2 ± 10.8	141.7 ± 10.7
Wrist Left	Front.	-29.6 ± 39.2	-28.3 ± 38.4	-27.9 ± 38.0	-28.5 ± 38.0	-28.9 ± 36.7	-29.1 ± 34.3	-27.8 ± 33.8	-25.4 ± 33.7	-21.1 ± 36.1	-24.5 ± 36.6	-25.0 ± 38.0	-27.9 ± 39.3
	Sag.	-1.9 ± 5.3	-1.8 ± 5.5	-1.9 ± 5.6	-1.8 ± 5.5	-1.9 ± 5.5	-1.9 ± 5.7	-1.9 ± 6.0	-1.4 ± 6.3	-1.2 ± 6.6	-1.1 ± 6.4	-0.4 ± 7.1	-1.5 ± 5.6
	Segm.	142.6 ± 10.0	142.4 ± 9.7	142.4 ± 9.6	142.3 ± 9.7	142.4 ± 9.6	142.8 ± 9.5	143.4 ± 9.7	144.3 ± 10.1	144.5 ± 10.3	144.4 ± 10.3	144.9 ± 10.5	143.4 ± 10.2

TABLE DII

MEAN CHARACTERISTIC ANGLES AND STANDARD DEVIATION OF LOWER EXTREMITIES FOR CITY BIKR AT EACH PEDAL ANGLE IN DEGREES

Pedal Angle [deg.]		0	30	60	90	120	150	180	210	240	270	300	330
Hip Right	Front.	24.0 ± 8.1	24.5 ± 7.7	17.4 ± 5.3	11.3 ± 3.5	9.2 ± 2.5	8.2 ± 2.1	7.7 ± 2.3	8.3 ± 2.5	8.6 ± 2.9	9.8 ± 2.1	12.7 ± 3.1	18.1 ± 5.0
	Sag.	22.2 ± 2.8	22.0 ± 2.7	28.3 ± 3.7	38.0 ± 4.1	48.0 ± 3.4	56.3 ± 3.2	59.5 ± 3.4	57.3 ± 2.7	52.8 ± 2.6	45.7 ± 2.6	37.7 ± 3.0	28.6 ± 2.9
Hip Left	Front.	8.2 ± 3.4	8.5 ± 3.9	9.3 ± 4.0	11.5 ± 4.4	14.6 ± 5.4	21.0 ± 6.7	26.8 ± 7.2	26.6 ± 8.5	20.2 ± 6.5	13.5 ± 4.2	10.3 ± 3.5	8.7 ± 3.3
	Sag.	60.4 ± 3.9	58.7 ± 3.5	54.1 ± 3.8	46.9 ± 3.3	38.5 ± 3.3	28.9 ± 4.0	22.1 ± 4.0	21.6 ± 4.2	27.2 ± 4.2	37.1 ± 4.0	48.3 ± 4.2	57.7 ± 4.4
Knee Right	Front.	-1.3 ± 4.0	-1.3 ± 3.0	-0.2 ± 2.0	1.4 ± 1.9	1.6 ± 1.8	1.3 ± 1.5	1.1 ± 1.6	0.8 ± 1.8	0.9 ± 2.3	0.6 ± 2.6	-0.1 ± 3.5	-1.0 ± 3.8
	Sag.	49.5 ± 4.4	59.8 ± 4.4	69.1 ± 4.6	75.9 ± 4.6	80.2 ± 4.5	80.5 ± 5.2	74.6 ± 5.0	63.9 ± 4.2	52.9 ± 4.2	43.9 ± 4.2	39.0 ± 4.7	41.0 ± 4.5
	Segm.	71.7 ± 4.4	81.6 ± 4.2	97.3 ± 6.5	113.7 ± 7.4	128.0 ± 6.6	136.5 ± 7.4	133.8 ± 7.8	120.9 ± 5.8	105.6 ± 5.1	89.6 ± 4.7	76.7 ± 4.2	69.7 ± 4.3
Knee Left	Front.	0.1 ± 2.8	-0.4 ± 3.2	-1.1 ± 3.3	-2.5 ± 4.1	-4.0 ± 4.8	-4.7 ± 4.1	-4.1 ± 3.9	-3.2 ± 4.1	-1.9 ± 3.2	-0.5 ± 2.6	-0.0 ± 2.6	0.2 ± 2.6
	Sag.	75.3 ± 4.1	65.1 ± 3.6	53.1 ± 3.7	43.9 ± 3.4	39.6 ± 3.1	42.0 ± 3.3	49.9 ± 3.6	60.2 ± 3.5	69.3 ± 3.2	76.3 ± 3.4	81.3 ± 3.8	81.8 ± 4.4
	Segm.	135.0 ± 7.1	123.2 ± 6.0	106.8 ± 5.6	90.5 ± 5.0	77.8 ± 4.3	70.6 ± 4.3	71.6 ± 4.3	81.4 ± 4.9	96.0 ± 5.4	113.0 ± 6.4	129.0 ± 7.4	138.8 ± 8.2
Ankle Right	Front.	-7.3 ± 5.6	-7.3 ± 9.4	-8.0 ± 15.1	-6.3 ± 23.4	-6.9 ± 15.9	-6.7 ± 9.4	-5.5 ± 6.8	-5.7 ± 5.1	-5.2 ± 4.7	-5.1 ± 4.1	-5.9 ± 4.0	-6.9 ± 4.2
	Sag.	34.5 ± 5.2	22.6 ± 5.6	13.8 ± 7.5	11.8 ± 7.3	15.9 ± 7.2	24.2 ± 7.0	35.5 ± 8.2	46.3 ± 6.1	54.3 ± 5.2	58.7 ± 6.3	54.8 ± 7.5	46.4 ± 5.4
	Segm.	84.0 ± 4.6	82.4 ± 5.2	82.9 ± 6.2	87.6 ± 4.7	96.0 ± 5.0	104.5 ± 5.4	110.0 ± 5.7	110.0 ± 5.4	107.0 ± 5.8	102.5 ± 6.7	93.7 ± 8.5	87.5 ± 5.4
Ankle Left	Front.	-10.2 ± 7.9	-8.1 ± 6.8	-6.8 ± 6.5	-6.4 ± 5.9	-7.2 ± 5.6	-8.3 ± 6.6	-8.7 ± 8.1	-11.2 ± 11.7	-16.3 ± 18.8	-19.3 ± 23.6	-15.3 ± 19.7	-11.7 ± 12.5
	Sag.	32.3 ± 5.4	41.7 ± 6.1	47.8 ± 8.6	52.8 ± 6.0	52.0 ± 5.8	46.3 ± 6.0	35.3 ± 6.0	23.0 ± 5.8	15.1 ± 6.6	11.2 ± 7.0	13.6 ± 6.7	20.8 ± 5.5
	Segm.	107.5 ± 4.2	106.7 ± 5.9	100.9 ± 8.6	96.8 ± 6.2	91.8 ± 6.4	88.6 ± 6.2	85.4 ± 5.8	83.4 ± 6.0	84.5 ± 6.0	87.5 ± 4.9	94.8 ± 4.1	102.5 ± 2.8

TABLE DIII

MEAN CHARACTERISTIC ANGLES AND STANDARD DEVIATION OF SPINE AND PELVIS FOR CITY BIKR AT EACH PEDAL ANGLE IN DEGREES

Pedal Angle [deg.]		0	30	60	90	120	150	180	210	240	270	300	330
T4	Front.	2.8 ± 4.2	3.4 ± 4.0	2.9 ± 4.0	2.0 ± 4.0	1.5 ± 4.4	-0.4 ± 3.4	-1.6 ± 3.7	-1.4 ± 4.4	-0.9 ± 4.5	-0.2 ± 4.2	0.7 ± 4.2	1.8 ± 4.2
	Sag.	44.5 ± 4.2	44.8 ± 4.3	45.5 ± 4.1	44.7 ± 4.6	45.8 ± 6.7	44.8 ± 4.7	44.8 ± 4.6	46.2 ± 6.3	45.1 ± 6.4	45.4 ± 6.3	45.3 ± 6.6	44.8 ± 4.4
T7	Front.	3.6 ± 5.6	3.9 ± 5.8	2.9 ± 5.6	1.6 ± 5.4	0.2 ± 5.1	-2.0 ± 5.0	-3.2 ± 3.8	-3.1 ± 4.1	-2.1 ± 3.9	-1.0 ± 4.2	0.6 ± 4.8	2.2 ± 5.6
	Sag.	37.8 ± 5.0	38.2 ± 5.0	38.6 ± 5.5	38.6 ± 5.8	37.0 ± 4.9	38.9 ± 5.0	37.8 ± 4.8	38.0 ± 6.5	37.2 ± 4.9	38.2 ± 6.4	38.2 ± 6.2	38.0 ± 4.8
T10	Front.	4.4 ± 3.0	4.7 ± 2.8	3.9 ± 2.5	2.8 ± 2.6	1.5 ± 2.5	-0.4 ± 2.7	-1.6 ± 2.5	-1.9 ± 2.8	-1.4 ± 2.8	-0.2 ± 2.4	1.3 ± 2.5	3.1 ± 3.2
	Sag.	24.5 ± 5.2	24.8 ± 4.9	24.6 ± 4.9	24.4 ± 4.8	24.9 ± 5.2	23.8 ± 5.6	24.5 ± 5.3	24.4 ± 4.9	25.0 ± 5.1	24.4 ± 4.5	24.4 ± 4.7	24.6 ± 5.1
T12	Front.	2.4 ± 4.4	2.7 ± 4.0	1.9 ± 3.6	0.8 ± 3.4	-0.7 ± 3.3	-2.6 ± 3.0	-3.9 ± 3.1	-4.3 ± 3.3	-3.6 ± 3.2	-2.8 ± 3.6	-1.2 ± 4.0	0.8 ± 4.6
	Sag.	20.4 ± 5.6	21.4 ± 6.0	21.8 ± 6.6	21.2 ± 5.9	21.0 ± 5.8	20.1 ± 5.5	19.7 ± 5.6	20.2 ± 5.7	20.3 ± 5.2	20.9 ± 5.8	21.7 ± 7.1	21.1 ± 6.6
L3	Front.	2.7 ± 4.4	2.9 ± 4.3	2.1 ± 4.0	1.4 ± 3.0	0.2 ± 2.6	-1.4 ± 2.6	-2.4 ± 1.9	-2.7 ± 2.0	-2.4 ± 2.0	-1.6 ± 2.2	-0.4 ± 3.1	1.4 ± 4.1
	Sag.	13.1 ± 6.1	13.3 ± 6.1	13.3 ± 6.2	13.4 ± 6.0	13.5 ± 6.0	13.0 ± 6.0	12.8 ± 6.0	13.1 ± 5.9	13.5 ± 5.8	13.1 ± 5.9	12.7 ± 6.0	12.8 ± 6.4
L5	Front.	1.6 ± 3.2	1.7 ± 3.4	1.7 ± 3.1	1.6 ± 2.7	1.3 ± 2.4	0.9 ± 2.1	0.4 ± 2.1	0.5 ± 2.2	0.5 ± 2.3	0.5 ± 2.5	0.6 ± 2.9	1.2 ± 3.1
	Sag.	5.6 ± 8.8	5.8 ± 8.8	5.9 ± 8.8	5.9 ± 8.6	5.9 ± 8.7	6.1 ± 9.5	5.5 ± 9.0	5.6 ± 9.1	5.9 ± 8.5	5.5 ± 8.8	5.5 ± 8.8	5.6 ± 9.1
Lumbar	Front.	2.1 ± 3.8	2.3 ± 3.8	1.9 ± 3.4	1.5 ± 2.7	0.7 ± 2.3	-0.4 ± 2.1	-1.3 ± 1.7	-1.4 ± 1.7	-1.2 ± 1.9	-0.7 ± 2.0	-0.0 ± 2.8	1.2 ± 3.5
	Sag.	9.9 ± 7.0	10.1 ± 7.1	10.2 ± 7.2	10.2 ± 7.0	10.2 ± 7.0	10.0 ± 7.4	9.6 ± 7.1	9.8 ± 7.1	10.2 ± 6.8	9.9 ± 7.0	9.6 ± 7.0	9.7 ± 7.4
Thoracic	Front.	3.4 ± 3.2	3.7 ± 3.0	2.9 ± 2.6	1.9 ± 2.6	0.6 ± 2.5	-1.3 ± 2.4	-2.6 ± 2.1	-2.7 ± 2.5	-2.0 ± 2.4	-1.0 ± 2.3	0.4 ± 2.6	2.1 ± 3.3
	Sag.	33.2 ± 3.4	33.6 ± 3.2	33.9 ± 3.3	33.5 ± 3.4	33.5 ± 3.4	33.2 ± 3.6	33.1 ± 3.8	33.5 ± 3.5	33.3 ± 3.5	33.5 ± 3.1	33.5 ± 3.3	33.4 ± 3.5
Cervical	Front.	-3.1 ± 6.9	-2.9 ± 6.7	-2.8 ± 6.7	-3.1 ± 6.2	-3.5 ± 6.2	-4.3 ± 6.1	-4.3 ± 6.3	-3.9 ± 5.6	-4.3 ± 7.1	-4.0 ± 7.5	-4.0 ± 7.7	-3.2 ± 7.1
	Sag.	9.0 ± 13.0	9.3 ± 13.2	9.5 ± 13.2	9.5 ± 13.2	9.6 ± 13.1	9.7 ± 13.2	9.7 ± 13.0	9.2 ± 13.2	10.3 ± 13.6	9.9 ± 13.1	10.7 ± 13.2	9.4 ± 13.1
Pelvis	Front.	-0.4 ± 3.1	-0.0 ± 3.4	0.2 ± 3.4	0.4 ± 3.1	0.4 ± 2.9	0.3 ± 2.7	0.1 ± 2.6	-0.1 ± 2.7	-0.2 ± 2.7	-0.4 ± 2.7	-0.4 ± 2.7	-0.4 ± 2.8
	Sag.	3.4 ± 7.2	3.4 ± 7.5	3.3 ± 7.5	2.9 ± 7.5	2.6 ± 7.7	1.7 ± 8.1	1.0 ± 8.0	1.1 ± 7.9	1.6 ± 7.8	2.2 ± 7.6	2.7 ± 7.6	3.4 ± 7.6

TABLE DIV

MEAN CHARACTERISTIC ANGLES AND STANDARD DEVIATION OF UPPER EXTREMITIES FOR RACING BIKR AT EACH PEDAL ANGLE IN DEGREES

Pedal Angle [deg.]		0	30	60	90	120	150	180	210	240	270	300	330
Shoulder Right	Front.	13.8 ± 5.2	13.6 ± 5.1	13.8 ± 5.0	14.2 ± 4.9	14.4 ± 4.8	14.8 ± 4.7	15.1 ± 4.6	15.6 ± 4.4	15.4 ± 4.5	15.0 ± 4.5	14.4 ± 5.1	13.8 ± 5.1
	Sag.	82.9 ± 4.4	82.8 ± 4.5	83.1 ± 4.5	83.4 ± 4.4	83.5 ± 4.5	83.6 ± 4.4	83.4 ± 4.5	83.4 ± 4.2	83.4 ± 4.3	83.4 ± 4.3	83.2 ± 4.4	82.9 ± 4.2
Shoulder Left	Front.	13.7 ± 7.1	14.1 ± 7.1	14.1 ± 7.2	13.6 ± 7.0	13.4 ± 7.2	12.8 ± 7.3	12.4 ± 7.4	12.0 ± 7.2	12.2 ± 7.2	12.3 ± 7.2	12.9 ± 6.8	13.6 ± 7.1
	Sag.	82.7 ± 5.6	82.7 ± 5.6	82.8 ± 5.6	82.8 ± 5.6	82.6 ± 5.6	82.5 ± 5.6	82.2 ± 5.8	82.2 ± 5.9	82.4 ± 5.9	82.5 ± 6.0	82.6 ± 5.9	82.8 ± 5.7
Elbow Right	Front.	-4.2 ± 5.4	-4.6 ± 5.4	-4.8 ± 5.3	-4.6 ± 5.3	-4.4 ± 5.2	-4.0 ± 5.3	-3.7 ± 5.4	-3.1 ± 5.4	-3.1 ± 5.4	-2.9 ± 5.3	-3.3 ± 5.1	-3.7 ± 5.1
	Sag.	40.6 ± 2.3	40.4 ± 2.2	40.2 ± 2.3	40.5 ± 2.4	40.7 ± 2.6	41.0 ± 2.6	41.1 ± 2.5	41.2 ± 2.5	41.0 ± 2.4	40.9 ± 2.5	40.8 ± 2.6	40.8 ± 2.6
	Segm.	133.9 ± 7.1	133.8 ± 7.2	133.3 ± 7.2	133.2 ± 7.2	133.2 ± 7.4	133.2 ± 7.4	133.5 ± 7.4	133.7 ± 7.2	133.6 ± 7.1	133.7 ± 7.1	133.8 ± 7.2	134.2 ± 7.1
Elbow Left	Front.	-2.8 ± 4.7	-2.6 ± 4.5	-2.7 ± 4.5	-2.8 ± 4.4	-2.9 ± 4.4	-3.1 ± 4.4	-3.3 ± 4.6	-4.0 ± 4.8	-4.0 ± 4.8	-3.9 ± 4.7	-3.5 ± 5.0	-3.1 ± 5.1
	Sag.	43.8 ± 3.3	43.8 ± 3.2	43.7 ± 3.2	43.7 ± 3.4	43.7 ± 3.4	43.6 ± 3.3	43.3 ± 3.2	43.1 ± 3.2	43.0 ± 3.3	43.1 ± 3.1	43.4 ± 3.2	43.7 ± 3.3
	Segm.	137.5 ± 8.8	137.3 ± 8.8	137.2 ± 8.8	137.4 ± 8.8	137.5 ± 8.7	137.7 ± 8.7	137.8 ± 8.8	137.6 ± 8.7	137.3 ± 8.7	137.3 ± 8.9	137.3 ± 9.1	137.2 ± 8.9
Wrist Right	Front.	40.7 ± 7.6	40.7 ± 7.5	40.5 ± 7.3	40.5 ± 7.3	40.7 ± 7.2	40.9 ± 7.4	40.9 ± 7.1	41.3 ± 7.2	41.3 ± 7.4	41.3 ± 7.5	41.2 ± 7.4	40.9 ± 7.5
	Sag.	-25.7 ± 5.8	-25.7 ± 5.8	-25.9 ± 5.9	-25.8 ± 5.7	-25.9 ± 5.8	-25.8 ± 5.8	-25.8 ± 5.8	-25.9 ± 5.7	-25.8 ± 6.0	-25.7 ± 6.0	-25.8 ± 6.0	-25.8 ± 5.9
	Segm.	111.2 ± 5.8	111.4 ± 5.9	111.2 ± 6.0	111.1 ± 6.2	110.9 ± 6.3	110.8 ± 6.4	110.7 ± 6.4	110.6 ± 6.3	110.9 ± 6.5	111.2 ± 6.3	111.1 ± 6.1	111.0 ± 5.9
Wrist Left	Front.	45.8 ± 12.5	45.5 ± 12.8	45.4 ± 12.9	45.4 ± 12.8	45.4 ± 12.8	45.2 ± 13.0	45.2 ± 13.0	45.2 ± 13.0	45.3 ± 13.0	45.6 ± 13.0	45.6 ± 12.9	45.8 ± 12.7
	Sag.	-21.7 ± 5.2	-21.9 ± 5.4	-21.9 ± 5.3	-21.8 ± 5.3	-21.8 ± 5.3	-21.8 ± 5.3	-21.7 ± 5.3	-21.7 ± 5.3	-21.7 ± 5.4	-21.6 ± 5.4	-21.7 ± 5.4	-21.7 ± 5.3
	Segm.	112.0 ± 6.1	112.0 ± 6.2	112.0 ± 6.2	112.1 ± 6.2	112.1 ± 6.2	112.1 ± 6.1	112.4 ± 6.0	112.5 ± 6.1	112.5 ± 6.0	112.5 ± 6.1	112.4 ± 6.2	112.1 ± 6.3

TABLE DV

MEAN CHARACTERISTIC ANGLES AND STANDARD DEVIATION OF LOWER EXTREMITIES FOR RACING BIKR AT EACH PEDAL ANGLE IN DEGREES

Pedal Angle [deg.]		0	30	60	90	120	150	180	210	240	270	300	330
Hip Right	Front.	17.3 ± 8.8	18.1 ± 8.1	12.9 ± 3.7	8.6 ± 2.9	7.7 ± 2.0	7.0 ± 1.9	6.4 ± 1.6	7.8 ± 2.2	8.3 ± 3.1	9.8 ± 3.9	11.8 ± 5.0	15.2 ± 6.3
	Sag.	23.7 ± 3.2	22.8 ± 3.4	28.6 ± 4.2	37.1 ± 4.0	47.2 ± 4.7	56.7 ± 6.1	61.3 ± 4.6	60.1 ± 3.6	56.2 ± 3.0	49.2 ± 3.4	40.4 ± 3.3	30.6 ± 2.9
Hip Left	Front.	6.6 ± 2.5	6.9 ± 3.1	7.8 ± 3.6	9.7 ± 3.2	12.1 ± 4.1	15.0 ± 6.3	19.9 ± 7.3	18.4 ± 6.2	13.2 ± 5.0	9.4 ± 3.9	7.3 ± 3.1	6.4 ± 2.5
	Sag.	61.8 ± 5.7	60.3 ± 4.7	55.7 ± 4.6	49.7 ± 4.3	41.9 ± 4.0	32.6 ± 4.0	24.7 ± 4.0	23.5 ± 4.2	28.5 ± 4.3	37.9 ± 4.5	48.9 ± 5.5	58.1 ± 6.2
Knee Right	Front.	-0.7 ± 4.2	-0.4 ± 3.4	0.7 ± 2.3	2.0 ± 2.1	1.9 ± 1.5	2.0 ± 1.8	1.8 ± 1.9	0.5 ± 2.4	-0.1 ± 2.9	-1.2 ± 3.5	-2.2 ± 4.8	-2.3 ± 4.5
	Sag.	47.7 ± 5.1	58.1 ± 5.6	67.9 ± 6.2	73.8 ± 5.0	78.2 ± 5.7	78.0 ± 4.6	73.8 ± 6.7	63.1 ± 5.4	52.0 ± 4.8	43.0 ± 4.5	38.0 ± 4.7	39.8 ± 4.9
	Segm.	71.4 ± 6.0	80.8 ± 6.6	96.4 ± 9.2	110.9 ± 7.9	125.3 ± 9.3	135.8 ± 11.9	135.0 ± 10.2	122.9 ± 7.9	108.0 ± 6.2	92.0 ± 5.2	78.2 ± 5.0	70.3 ± 5.6
Knee Left	Front.	0.3 ± 2.1	-0.4 ± 2.9	-1.0 ± 3.9	-2.5 ± 4.4	-4.2 ± 5.6	-4.0 ± 6.1	-3.7 ± 4.3	-2.0 ± 3.6	-0.2 ± 3.3	0.8 ± 2.9	1.3 ± 2.4	1.2 ± 2.0
	Sag.	71.2 ± 6.9	61.0 ± 5.7	49.4 ± 5.8	41.0 ± 5.1	35.8 ± 4.5	37.0 ± 4.4	45.1 ± 4.3	55.9 ± 4.1	65.4 ± 4.3	72.4 ± 5.0	76.6 ± 5.6	75.9 ± 4.7
	Segm.	132.7 ± 12.3	120.9 ± 9.8	104.8 ± 9.1	90.4 ± 7.5	77.4 ± 6.3	69.3 ± 6.0	69.5 ± 6.2	79.2 ± 6.6	93.8 ± 7.4	110.2 ± 8.8	125.4 ± 11.1	134.8 ± 13.3
Ankle Right	Front.	-5.0 ± 8.0	-4.5 ± 14.5	-4.8 ± 33.6	-11.7 ± 31.4	-14.3 ± 19.1	-12.2 ± 12.9	-9.1 ± 7.4	-7.1 ± 5.2	-5.7 ± 5.0	-5.5 ± 4.9	-5.1 ± 5.0	-5.1 ± 6.1
	Sag.	37.0 ± 6.8	24.3 ± 7.4	16.0 ± 8.3	13.0 ± 8.8	15.9 ± 7.2	22.1 ± 6.6	32.6 ± 6.7	44.7 ± 5.2	52.2 ± 5.0	58.3 ± 8.4	57.3 ± 8.1	49.3 ± 7.4
	Segm.	84.7 ± 5.1	82.4 ± 5.3	83.8 ± 5.8	86.7 ± 7.3	93.9 ± 6.7	101.0 ± 7.1	106.2 ± 8.4	107.6 ± 7.3	104.2 ± 6.7	101.3 ± 10.0	95.4 ± 9.2	89.2 ± 6.1
Ankle Left	Front.	-9.8 ± 10.8	-7.6 ± 8.4	-6.5 ± 7.8	-6.7 ± 7.2	-6.6 ± 7.6	-7.0 ± 7.6	-6.8 ± 8.1	-8.2 ± 11.6	-13.4 ± 15.3	-20.2 ± 17.3	-18.3 ± 15.6	-13.6 ± 13.3
	Sag.	34.5 ± 9.8	46.7 ± 9.6	55.8 ± 9.9	60.5 ± 10.4	59.0 ± 10.1	53.0 ± 9.6	41.2 ± 9.7	27.4 ± 10.2	19.9 ± 10.8	17.1 ± 10.4	18.8 ± 10.4	24.9 ± 9.9
	Segm.	105.3 ± 7.1	107.3 ± 8.1	104.9 ± 10.1	101.3 ± 10.4	94.7 ± 8.6	89.9 ± 7.3	86.3 ± 7.0	83.2 ± 7.6	85.1 ± 7.9	89.3 ± 7.7	95.2 ± 7.3	101.5 ± 7.0

TABLE DVI

MEAN CHARACTERISTIC ANGLES AND STANDARD DEVIATION OF SPINE AND PELVIS FOR RACING BIKR AT EACH PEDAL ANGLE IN DEGREES

Pedal Angle [deg.]		0	30	60	90	120	150	180	210	240	270	300	330
T4	Front.	20.1 ± 29.8	21.5 ± 27.7	18.7 ± 28.8	13.0 ± 30.4	10.0 ± 28.4	2.7 ± 27.6	-5.7 ± 26.3	-6.5 ± 25.5	-2.1 ± 26.6	-0.3 ± 26.3	11.3 ± 33.4	18.5 ± 30.1
	Sag.	83.3 ± 4.2	83.5 ± 4.2	83.5 ± 4.2	83.5 ± 4.3	83.6 ± 4.4	83.6 ± 4.4	83.6 ± 4.3	83.6 ± 4.3	83.7 ± 4.3	82.2 ± 4.6	83.5 ± 4.5	83.1 ± 4.3
T7	Front.	8.6 ± 11.5	11.5 ± 14.1	9.9 ± 13.0	5.9 ± 11.2	4.1 ± 11.9	0.5 ± 11.1	-2.6 ± 10.5	-3.7 ± 10.8	-2.8 ± 12.3	-0.0 ± 11.3	4.2 ± 10.2	7.3 ± 11.0
	Sag.	70.0 ± 4.9	71.4 ± 5.9	71.4 ± 5.9	71.2 ± 6.0	71.2 ± 6.2	71.3 ± 6.3	71.4 ± 6.2	71.6 ± 6.1	71.6 ± 6.2	71.4 ± 6.1	71.3 ± 6.0	69.8 ± 4.8
T10	Front.	9.4 ± 9.9	9.7 ± 9.5	8.2 ± 9.5	4.8 ± 8.3	2.6 ± 8.6	-0.8 ± 8.4	-4.1 ± 9.4	-4.8 ± 8.8	-3.1 ± 7.7	-0.7 ± 7.2	3.0 ± 7.4	7.3 ± 9.3
	Sag.	66.7 ± 7.0	66.9 ± 6.9	66.9 ± 6.9	66.8 ± 6.9	66.8 ± 6.9	66.8 ± 6.9	66.9 ± 6.9	67.0 ± 6.9	67.1 ± 7.0	67.0 ± 7.0	66.8 ± 7.0	66.6 ± 7.1
T12	Front.	4.0 ± 9.8	4.3 ± 9.5	2.7 ± 9.2	-0.2 ± 8.8	-2.3 ± 8.4	-4.9 ± 7.8	-7.5 ± 6.7	-7.9 ± 7.2	-6.5 ± 8.3	-4.4 ± 8.4	-1.6 ± 8.0	1.9 ± 8.9
	Sag.	60.2 ± 7.3	60.4 ± 7.3	60.5 ± 7.2	60.5 ± 7.3	60.4 ± 7.2	60.2 ± 7.0	60.1 ± 6.9	60.3 ± 7.0	60.5 ± 7.0	60.5 ± 7.2	60.4 ± 7.2	60.1 ± 7.4
L3	Front.	2.3 ± 5.5	2.4 ± 5.7	1.5 ± 5.1	-0.3 ± 4.9	-1.8 ± 4.6	-3.3 ± 4.7	-5.0 ± 4.5	-5.1 ± 4.3	-4.2 ± 4.4	-2.8 ± 4.5	-1.1 ± 4.8	1.0 ± 5.2
	Sag.	50.2 ± 5.6	50.3 ± 5.6	50.6 ± 5.6	50.7 ± 5.8	50.4 ± 5.8	50.2 ± 5.7	50.0 ± 5.7	50.1 ± 5.6	50.5 ± 5.7	50.5 ± 5.8	50.4 ± 5.8	50.2 ± 5.7
L5	Front.	1.2 ± 3.8	1.4 ± 3.8	1.0 ± 3.6	0.6 ± 3.7	0.1 ± 3.7	-0.2 ± 3.8	-0.8 ± 3.5	-0.6 ± 3.4	-0.3 ± 3.5	0.2 ± 3.4	0.5 ± 3.0	0.9 ± 3.2
	Sag.	37.2 ± 5.9	37.3 ± 5.7	37.8 ± 5.8	37.7 ± 5.8	37.7 ± 5.9	37.4 ± 5.9	37.1 ± 5.8	37.1 ± 5.6	37.6 ± 5.5	37.5 ± 5.7	37.4 ± 5.5	37.3 ± 5.7
Lumbar	Front.	1.8 ± 4.2	1.9 ± 4.4	1.2 ± 3.9	0.1 ± 3.8	-0.9 ± 3.6	-1.9 ± 3.8	-3.1 ± 3.3	-3.0 ± 3.0	-2.3 ± 3.1	-1.4 ± 3.1	-0.4 ± 3.1	0.9 ± 3.5
	Sag.	44.4 ± 5.2	44.6 ± 5.1	44.9 ± 5.3	44.9 ± 5.5	44.8 ± 5.5	44.5 ± 5.4	44.3 ± 5.3	44.3 ± 5.1	44.7 ± 5.2	44.7 ± 5.4	44.6 ± 5.4	44.5 ± 5.2
Thoracic	Front.	9.2 ± 8.4	9.8 ± 8.0	8.0 ± 7.4	3.9 ± 5.4	1.5 ± 5.2	-2.0 ± 4.6	-5.4 ± 5.1	-6.1 ± 5.2	-4.3 ± 6.3	-1.8 ± 5.9	2.5 ± 4.6	7.1 ± 7.4
	Sag.	72.6 ± 3.4	72.7 ± 3.3	72.8 ± 3.3	72.5 ± 3.5	72.6 ± 3.6	72.5 ± 3.6	72.6 ± 3.6	72.8 ± 3.5	72.9 ± 3.5	73.2 ± 4.4	72.6 ± 3.6	72.5 ± 3.5
Cervical	Front.	0.0 ± 5.5	-0.3 ± 5.1	-0.5 ± 4.9	-1.9 ± 4.3	-2.8 ± 4.2	-3.8 ± 5.3	-4.4 ± 6.3	-4.3 ± 5.4	-4.1 ± 5.0	-2.5 ± 3.3	-1.8 ± 3.6	0.1 ± 5.6
	Sag.	33.6 ± 18.9	33.8 ± 19.0	34.0 ± 19.0	33.4 ± 19.0	33.6 ± 19.1	33.7 ± 19.1	33.8 ± 19.1	34.3 ± 18.9	34.5 ± 18.9	33.4 ± 17.0	33.9 ± 18.7	33.4 ± 18.9
Pelvis	Front.	-2.1 ± 3.8	-1.8 ± 3.5	-1.0 ± 3.2	0.2 ± 2.6	1.4 ± 2.6	2.6 ± 2.4	3.6 ± 2.2	3.1 ± 2.4	2.6 ± 2.4	1.5 ± 2.1	0.3 ± 2.4	-1.3 ± 3.8
	Sag.	33.4 ± 4.9	33.4 ± 5.1	33.7 ± 5.1	33.5 ± 5.2	32.9 ± 5.7	32.0 ± 5.5	30.9 ± 6.1	30.8 ± 6.3	31.6 ± 6.2	32.2 ± 5.9	32.9 ± 5.5	33.5 ± 5.1

TABLE DVII

MEAN CHARACTERISTIC ANGLES AND STANDARD DEVIATION OF UPPER EXTREMITIES FOR MOUNTAIN BIKR AT EACH PEDAL ANGLE IN DEGREES

Pedal Angle [deg.]		0	30	60	90	120	150	180	210	240	270	300	330
Shoulder Right	Front.	22.0 ± 3.9	21.8 ± 3.9	22.0 ± 3.8	22.2 ± 3.6	22.5 ± 3.6	22.8 ± 3.6	23.1 ± 3.6	23.3 ± 3.6	23.2 ± 3.5	22.9 ± 3.6	22.5 ± 3.7	22.3 ± 3.7
	Sag.	67.0 ± 6.9	66.9 ± 7.0	66.9 ± 6.9	67.0 ± 6.9	67.3 ± 6.9	67.4 ± 6.9	67.2 ± 6.9	67.2 ± 6.9	67.2 ± 6.9	67.2 ± 6.9	67.2 ± 6.9	67.2 ± 6.9
Shoulder Left	Front.	22.1 ± 6.3	22.3 ± 6.4	22.2 ± 6.4	22.0 ± 6.5	21.6 ± 6.4	21.4 ± 6.4	21.0 ± 6.4	20.8 ± 6.3	21.1 ± 6.5	21.3 ± 6.6	21.6 ± 6.5	21.8 ± 6.3
	Sag.	66.7 ± 6.7	66.6 ± 6.7	66.6 ± 6.6	66.6 ± 6.6	66.6 ± 6.6	66.5 ± 6.5	66.4 ± 6.7	66.5 ± 6.8	66.6 ± 6.8	66.7 ± 6.9	67.0 ± 6.8	67.0 ± 6.7
Elbow Right	Front.	-0.9 ± 3.6	-0.7 ± 3.4	-0.7 ± 3.5	-0.5 ± 3.7	-0.2 ± 3.7	0.0 ± 3.6	0.4 ± 3.9	0.3 ± 4.0	0.0 ± 4.0	-0.2 ± 3.9	-0.5 ± 3.7	-0.8 ± 3.7
	Sag.	39.0 ± 3.9	38.7 ± 3.9	38.8 ± 3.9	39.2 ± 3.8	39.5 ± 3.9	39.7 ± 3.8	39.7 ± 3.9	39.7 ± 3.8	39.5 ± 3.8	39.4 ± 3.7	39.4 ± 3.7	39.3 ± 3.8
	Segm.	145.4 ± 7.4	145.5 ± 7.4	145.4 ± 7.4	145.6 ± 7.6	145.6 ± 7.7	145.5 ± 7.5	145.6 ± 7.5	145.5 ± 7.5	145.4 ± 7.5	145.3 ± 7.5	145.4 ± 7.5	145.4 ± 7.5
Elbow Left	Front.	2.0 ± 3.9	2.0 ± 3.9	1.8 ± 3.8	1.7 ± 3.7	1.5 ± 3.6	1.3 ± 3.6	0.9 ± 3.8	1.0 ± 4.1	1.1 ± 3.9	1.3 ± 3.7	1.6 ± 3.7	1.9 ± 3.7
	Sag.	43.2 ± 4.9	43.2 ± 4.9	43.2 ± 5.0	43.2 ± 5.1	43.2 ± 5.0	43.0 ± 5.0	42.6 ± 5.1	42.5 ± 5.1	42.7 ± 5.1	42.9 ± 5.1	43.2 ± 5.0	43.2 ± 4.9
	Segm.	148.9 ± 6.6	148.9 ± 6.5	148.8 ± 6.4	149.0 ± 6.5	149.0 ± 6.4	149.0 ± 6.3	148.8 ± 6.4	148.9 ± 6.4	148.9 ± 6.4	148.8 ± 6.5	148.8 ± 6.7	148.8 ± 6.6
Wrist Right	Front.	-71.0 ± 11.1	-70.9 ± 11.0	-70.8 ± 10.9	-70.8 ± 10.8	-70.6 ± 11.0	-70.7 ± 11.2	-70.6 ± 10.9	-70.8 ± 11.1	-70.8 ± 10.7	-70.9 ± 10.8	-71.0 ± 10.9	-70.9 ± 11.0
	Sag.	10.0 ± 10.4	9.9 ± 10.4	10.0 ± 10.6	10.1 ± 10.6	10.1 ± 10.7	10.2 ± 10.6	10.1 ± 10.9	9.9 ± 10.9	9.8 ± 10.8	9.9 ± 10.7	9.9 ± 10.8	9.9 ± 10.8
	Segm.	136.5 ± 10.0	136.6 ± 10.1	136.6 ± 10.0	136.2 ± 10.1	135.9 ± 10.2	135.8 ± 10.3	135.4 ± 10.3	135.4 ± 10.4	135.5 ± 10.3	135.7 ± 10.3	135.8 ± 10.3	136.0 ± 10.2
Wrist Left	Front.	-75.2 ± 8.2	-75.0 ± 7.9	-75.0 ± 7.9	-75.1 ± 8.1	-75.1 ± 8.2	-75.1 ± 8.1	-75.1 ± 8.1	-75.4 ± 8.9	-75.2 ± 9.2	-75.2 ± 9.2	-75.3 ± 9.0	-75.4 ± 9.1
	Sag.	5.1 ± 10.9	5.1 ± 10.9	5.1 ± 11.0	5.2 ± 10.9	5.2 ± 11.0	5.1 ± 10.9	5.1 ± 10.8	4.9 ± 10.9	4.9 ± 11.1	4.9 ± 11.2	4.9 ± 11.1	5.0 ± 11.0
	Segm.	129.8 ± 8.9	129.8 ± 8.9	129.8 ± 8.9	129.9 ± 8.9	130.1 ± 8.9	130.2 ± 8.9	130.9 ± 9.1	130.8 ± 9.3	130.5 ± 9.5	130.3 ± 9.3	130.0 ± 9.3	129.8 ± 9.1

TABLE DVIII

MEAN CHARACTERISTIC ANGLES AND STANDARD DEVIATION OF LOWER EXTREMITIES FOR MOUNTAIN BIKR AT EACH PEDAL ANGLE IN DEGREES

Pedal Angle [deg.]		0	30	60	90	120	150	180	210	240	270	300	330
Hip Right	Front.	28.3 ± 7.6	29.3 ± 8.3	19.9 ± 5.1	12.0 ± 3.3	8.5 ± 2.5	8.0 ± 1.7	8.2 ± 1.7	8.6 ± 1.7	9.7 ± 2.2	11.4 ± 2.8	15.1 ± 3.8	20.4 ± 4.7
	Sag.	16.0 ± 3.5	15.7 ± 3.7	21.5 ± 3.8	31.6 ± 4.0	42.1 ± 4.3	50.4 ± 4.2	53.2 ± 3.7	52.4 ± 3.4	48.5 ± 3.2	42.1 ± 3.2	33.1 ± 3.1	22.9 ± 3.1
Hip Left	Front.	9.0 ± 4.4	9.5 ± 5.0	11.0 ± 5.8	13.1 ± 6.7	17.4 ± 8.0	25.6 ± 11.2	35.0 ± 15.4	34.3 ± 16.4	24.5 ± 11.2	16.1 ± 6.5	11.5 ± 5.0	9.7 ± 4.3
	Sag.	53.5 ± 4.4	52.7 ± 4.1	48.7 ± 4.1	42.2 ± 4.5	32.8 ± 5.0	22.4 ± 4.8	15.5 ± 5.0	15.5 ± 5.2	21.4 ± 5.0	31.3 ± 5.1	41.6 ± 5.6	50.3 ± 5.3
Knee Right	Front.	-2.9 ± 3.7	-2.7 ± 3.5	-1.0 ± 1.6	0.6 ± 1.7	1.4 ± 1.7	1.1 ± 1.3	0.4 ± 1.4	0.0 ± 1.6	-0.6 ± 2.2	-1.3 ± 3.3	-2.9 ± 4.1	-3.0 ± 3.5
	Sag.	50.1 ± 3.9	60.8 ± 3.9	69.4 ± 3.9	75.7 ± 4.1	78.8 ± 4.5	77.4 ± 4.5	71.0 ± 4.1	60.9 ± 4.1	49.7 ± 4.3	40.7 ± 4.3	36.8 ± 4.1	40.4 ± 3.7
	Segm.	66.0 ± 4.7	76.1 ± 5.2	90.7 ± 5.8	107.2 ± 6.8	120.8 ± 7.7	127.6 ± 7.7	123.9 ± 6.5	113.1 ± 5.6	98.0 ± 4.7	82.7 ± 4.1	69.8 ± 4.0	63.3 ± 4.1
Knee Left	Front.	-0.1 ± 2.9	-1.0 ± 3.4	-2.4 ± 4.0	-3.8 ± 4.7	-5.3 ± 4.9	-5.8 ± 4.8	-5.0 ± 4.2	-3.7 ± 4.0	-2.3 ± 3.4	-1.2 ± 3.0	-0.1 ± 2.6	0.1 ± 2.7
	Sag.	70.5 ± 3.7	60.5 ± 3.7	49.6 ± 3.7	40.3 ± 3.8	37.0 ± 4.1	41.0 ± 3.9	50.9 ± 3.9	61.4 ± 3.7	69.9 ± 3.6	75.9 ± 3.6	78.7 ± 3.8	77.6 ± 4.0
	Segm.	123.4 ± 6.7	112.6 ± 6.0	97.7 ± 5.3	82.1 ± 4.7	69.5 ± 4.4	63.2 ± 4.4	66.0 ± 4.8	76.4 ± 5.4	90.8 ± 6.2	106.6 ± 6.9	119.8 ± 8.2	127.3 ± 8.2
Ankle Right	Front.	-7.0 ± 8.4	-8.3 ± 16.0	-15.2 ± 40.5	-14.1 ± 34.1	-22.8 ± 26.9	-15.9 ± 11.2	-9.7 ± 8.0	-7.9 ± 6.1	-7.2 ± 5.4	-7.1 ± 4.8	-7.2 ± 4.6	-7.3 ± 5.1
	Sag.	32.7 ± 8.0	21.5 ± 8.4	14.3 ± 8.4	11.6 ± 9.4	14.4 ± 8.8	21.0 ± 8.3	32.6 ± 7.3	42.0 ± 7.0	49.8 ± 6.2	54.2 ± 6.3	52.6 ± 6.9	45.2 ± 6.9
	Segm.	82.8 ± 7.3	82.4 ± 7.3	83.7 ± 7.3	87.2 ± 7.7	92.9 ± 7.4	98.1 ± 7.3	103.4 ± 7.3	102.8 ± 7.9	99.5 ± 7.9	95.0 ± 8.0	89.5 ± 7.6	85.8 ± 6.4
Ankle Left	Front.	-13.1 ± 7.5	-9.9 ± 6.1	-8.6 ± 5.1	-8.2 ± 4.6	-8.9 ± 4.3	-9.8 ± 4.6	-11.5 ± 6.7	-16.5 ± 11.0	-26.4 ± 13.5	-32.8 ± 19.6	-27.7 ± 15.3	-18.9 ± 10.7
	Sag.	30.9 ± 5.3	40.8 ± 5.5	48.6 ± 5.4	51.8 ± 6.0	52.0 ± 6.3	45.0 ± 4.7	32.7 ± 5.3	21.3 ± 6.2	14.6 ± 6.4	12.2 ± 6.4	14.7 ± 6.7	20.9 ± 6.1
	Segm.	101.3 ± 5.0	101.4 ± 6.1	98.3 ± 6.2	92.4 ± 7.5	89.5 ± 7.9	86.6 ± 5.4	84.2 ± 5.5	83.2 ± 6.0	84.8 ± 5.6	88.2 ± 5.2	93.4 ± 4.6	98.4 ± 4.1

TABLE DIX

MEAN CHARACTERISTIC ANGLES AND STANDARD DEVIATION OF SPINE AND PELVIS FOR MOUNTAIN BIKR AT EACH PEDAL ANGLE IN DEGREES

Pedal Angle [deg.]		0	30	60	90	120	150	180	210	240	270	300	330
T4	Front.	3.0 ± 6.9	3.3 ± 5.8	2.6 ± 6.4	1.5 ± 6.7	0.4 ± 6.8	-0.6 ± 6.9	-1.8 ± 7.3	-2.2 ± 7.8	-1.0 ± 8.1	-0.2 ± 7.5	1.0 ± 7.0	1.7 ± 6.5
	Sag.	64.7 ± 5.2	64.7 ± 5.1	64.8 ± 5.1	64.6 ± 5.2	64.4 ± 5.2	64.4 ± 5.1	64.6 ± 5.1	64.7 ± 5.1	64.7 ± 5.0	64.6 ± 5.1	64.5 ± 5.1	64.5 ± 5.1
T7	Front.	3.6 ± 10.7	4.1 ± 11.0	3.2 ± 10.5	1.8 ± 10.3	-0.1 ± 10.4	-1.8 ± 10.4	-3.5 ± 10.6	-3.8 ± 10.8	-2.5 ± 10.5	-1.4 ± 10.8	0.3 ± 10.6	1.8 ± 10.7
	Sag.	59.7 ± 4.6	59.8 ± 4.4	59.9 ± 4.5	59.7 ± 4.6	59.5 ± 4.6	59.6 ± 4.5	59.6 ± 4.4	59.7 ± 4.3	59.6 ± 4.3	59.4 ± 4.3	59.4 ± 4.2	59.4 ± 4.2
T10	Front.	4.0 ± 5.2	4.2 ± 4.9	3.4 ± 4.4	2.3 ± 4.1	0.9 ± 4.0	-0.5 ± 4.3	-2.1 ± 5.0	-2.4 ± 5.0	-1.3 ± 4.7	-0.3 ± 4.5	1.1 ± 4.3	2.5 ± 4.6
	Sag.	44.7 ± 8.3	44.9 ± 8.3	44.7 ± 8.3	44.4 ± 8.5	44.4 ± 8.5	44.5 ± 8.4	44.9 ± 8.1	45.1 ± 8.0	45.1 ± 8.1	44.9 ± 8.2	44.7 ± 8.0	44.6 ± 8.1
T12	Front.	1.2 ± 5.9	1.5 ± 6.2	0.7 ± 6.0	-0.4 ± 5.5	-2.1 ± 4.7	-3.7 ± 4.4	-5.3 ± 3.9	-5.2 ± 4.2	-4.2 ± 4.5	-3.2 ± 4.4	-1.8 ± 4.6	-0.4 ± 5.1
	Sag.	40.2 ± 8.7	40.3 ± 8.9	40.3 ± 9.1	40.2 ± 9.0	40.0 ± 8.8	40.0 ± 8.8	40.2 ± 8.8	40.4 ± 8.8	40.3 ± 8.9	40.2 ± 8.8	40.1 ± 8.6	40.1 ± 8.6
L3	Front.	1.2 ± 4.4	1.2 ± 4.4	0.5 ± 4.0	-0.4 ± 3.4	-1.4 ± 3.1	-2.6 ± 2.8	-3.7 ± 2.8	-3.5 ± 2.6	-2.8 ± 2.6	-2.1 ± 3.1	-0.8 ± 3.1	0.3 ± 4.0
	Sag.	31.6 ± 8.5	31.6 ± 8.5	31.5 ± 8.4	31.6 ± 8.3	31.6 ± 8.3	31.7 ± 8.3	31.7 ± 8.4	31.7 ± 8.3	31.7 ± 8.3	31.7 ± 8.4	31.6 ± 8.5	31.6 ± 8.5
L5	Front.	0.6 ± 3.0	0.2 ± 2.9	-0.0 ± 2.6	-0.0 ± 2.5	-0.4 ± 2.4	-0.6 ± 2.3	-1.0 ± 1.9	-0.5 ± 2.1	-0.5 ± 2.3	-0.3 ± 2.5	0.0 ± 2.5	0.4 ± 2.8
	Sag.	21.3 ± 9.1	21.3 ± 9.0	21.3 ± 9.1	21.7 ± 9.5	21.5 ± 8.9	21.8 ± 9.3	21.8 ± 9.0	21.8 ± 8.9	22.0 ± 9.1	21.6 ± 8.9	21.5 ± 9.0	21.5 ± 9.1
Lumbar	Front.	0.9 ± 3.5	0.7 ± 3.5	0.2 ± 3.1	-0.2 ± 2.6	-1.0 ± 2.4	-1.7 ± 2.1	-2.5 ± 1.9	-2.1 ± 1.8	-1.8 ± 2.1	-1.3 ± 2.4	-0.5 ± 2.4	0.3 ± 3.1
	Sag.	26.9 ± 8.5	26.9 ± 8.5	26.9 ± 8.5	27.1 ± 8.6	27.1 ± 8.4	27.2 ± 8.6	27.2 ± 8.4	27.2 ± 8.4	27.3 ± 8.4	27.1 ± 8.4	27.1 ± 8.5	27.1 ± 8.6
Thoracic	Front.	2.9 ± 5.2	3.2 ± 4.9	2.4 ± 4.7	1.2 ± 4.6	-0.3 ± 4.5	-1.7 ± 4.6	-3.2 ± 5.0	-3.5 ± 5.2	-2.3 ± 5.1	-1.4 ± 4.8	0.1 ± 4.6	1.3 ± 4.7
	Sag.	53.6 ± 4.4	53.7 ± 4.3	53.7 ± 4.4	53.5 ± 4.5	53.3 ± 4.4	53.4 ± 4.4	53.6 ± 4.4	53.7 ± 4.4	53.7 ± 4.4	53.5 ± 4.4	53.4 ± 4.3	53.4 ± 4.2
Cervical	Front.	-0.7 ± 5.0	-0.6 ± 4.9	-0.8 ± 4.8	-1.3 ± 4.8	-1.8 ± 4.8	-2.2 ± 4.7	-2.1 ± 4.5	-1.9 ± 4.2	-1.4 ± 4.2	-1.6 ± 4.6	-1.3 ± 4.6	-1.4 ± 4.7
	Sag.	26.3 ± 15.9	26.3 ± 15.8	26.1 ± 15.8	26.1 ± 15.9	26.1 ± 16.1	26.2 ± 16.2	26.3 ± 16.1	26.2 ± 16.3	26.3 ± 16.2	26.4 ± 16.2	26.4 ± 16.2	26.6 ± 16.3
Pelvis	Front.	-1.9 ± 3.6	-1.9 ± 3.8	-1.4 ± 3.8	-0.8 ± 3.9	-0.0 ± 4.0	0.6 ± 4.5	1.3 ± 4.0	1.4 ± 4.1	0.9 ± 4.0	-0.1 ± 4.7	-0.5 ± 3.8	-1.2 ± 3.6
	Sag.	17.2 ± 8.2	17.2 ± 8.1	17.1 ± 8.0	16.9 ± 8.2	16.4 ± 8.3	15.7 ± 8.6	14.9 ± 8.7	14.8 ± 8.6	15.5 ± 8.6	16.5 ± 8.7	17.1 ± 8.5	17.5 ± 8.5

TABLE DX

MEAN SEGMENT LENGTHS AND STANDARD DEVIATION OF UPPER EXTREMITIES FOR CITY BIKE AT EACH PEDAL ANGLE IN MM

	Pedal Angle [deg.]	0	30	60	90	120	150	180	210	240	270	300	330
Right Side	SH-C7	216.6 ± 31.2	216.8 ± 31.9	215.3 ± 31.4	215.9 ± 32.7	215.5 ± 32.6	215.4 ± 32.8	215.3 ± 32.4	214.4 ± 32.3	215.5 ± 30.6	215.9 ± 30.8	216.3 ± 30.2	215.8 ± 31.4
	SH-EL	267.9 ± 20.7	267.8 ± 20.7	268.0 ± 20.9	268.1 ± 21.0	268.2 ± 21.1	268.4 ± 21.2	268.3 ± 21.1	268.3 ± 20.9	267.9 ± 21.0	268.0 ± 20.4	267.7 ± 20.7	268.0 ± 20.5
	EL-WR	263.4 ± 8.0	263.5 ± 8.0	263.5 ± 7.9	263.5 ± 8.0	263.6 ± 8.0	263.5 ± 8.1	263.5 ± 8.1	263.5 ± 8.0	263.4 ± 8.0	263.4 ± 7.9	263.3 ± 7.9	263.4 ± 8.0
	WR-FI	85.5 ± 4.5	85.8 ± 4.6	85.7 ± 4.4	85.7 ± 4.4	85.5 ± 4.4	85.1 ± 4.3	84.8 ± 4.4	84.7 ± 4.3	84.7 ± 4.4	84.8 ± 4.5	84.9 ± 4.5	85.2 ± 4.6
	SH-SS	159.2 ± 17.9	159.0 ± 18.4	158.8 ± 18.7	158.5 ± 18.8	158.4 ± 18.7	158.4 ± 18.5	158.4 ± 18.4	158.4 ± 18.7	158.6 ± 18.4	158.8 ± 18.3	159.2 ± 18.2	159.1 ± 17.5
	SH-SI	205.5 ± 11.9	205.5 ± 12.7	205.3 ± 13.0	204.9 ± 13.1	204.3 ± 13.0	203.9 ± 12.7	203.6 ± 12.6	203.6 ± 12.3	203.7 ± 11.9	204.2 ± 11.4	205.0 ± 11.4	205.1 ± 11.6
Left Side	SH-C7	215.0 ± 34.0	214.6 ± 34.1	213.4 ± 33.4	214.5 ± 33.8	214.3 ± 33.7	214.7 ± 33.7	215.7 ± 33.6	215.4 ± 34.4	215.9 ± 33.0	215.7 ± 33.3	215.3 ± 32.9	214.8 ± 33.9
	SH-EL	268.3 ± 22.9	268.4 ± 22.9	268.3 ± 23.0	268.1 ± 22.8	267.7 ± 22.6	267.4 ± 22.5	267.3 ± 22.6	267.6 ± 23.0	267.5 ± 22.9	267.7 ± 22.9	267.9 ± 22.9	268.1 ± 22.9
	EL-WR	264.4 ± 10.2	264.4 ± 10.2	264.4 ± 10.2	264.4 ± 10.2	264.4 ± 10.1	264.4 ± 10.0	264.5 ± 10.1	264.5 ± 10.2	264.5 ± 10.3	264.4 ± 10.2	264.5 ± 10.4	264.5 ± 10.2
	WR-FI	84.4 ± 7.3	84.3 ± 7.3	84.4 ± 7.3	84.3 ± 7.3	84.3 ± 7.3	84.5 ± 7.3	84.9 ± 7.3	85.2 ± 7.2	85.2 ± 7.2	85.1 ± 7.1	85.1 ± 7.1	84.7 ± 7.3
	SH-SS	158.3 ± 18.1	158.5 ± 18.0	158.7 ± 18.0	158.9 ± 17.8	159.1 ± 17.8	159.5 ± 17.7	159.7 ± 18.0	159.7 ± 18.3	159.4 ± 18.3	159.0 ± 17.9	158.8 ± 18.1	158.5 ± 18.1
	SH-SI	200.7 ± 5.5	200.6 ± 5.3	201.1 ± 5.4	201.9 ± 5.4	202.2 ± 5.4	203.0 ± 5.7	203.7 ± 6.0	204.0 ± 6.2	203.7 ± 6.2	203.1 ± 6.2	202.4 ± 6.0	201.5 ± 5.7

TABLE DXI

MEAN SEGMENT LENGTHS AND STANDARD DEVIATION OF LOWER EXTREMITIES FOR CITY BIKE AT EACH PEDAL ANGLE IN MM

	Pedal Angle [deg.]	0	30	60	90	120	150	180	210	240	270	300	330
Right Side	HI-PSIS	146.0 ± 12.8	145.8 ± 12.7	147.8 ± 13.7	149.7 ± 14.7	148.8 ± 15.1	146.0 ± 15.4	145.0 ± 15.5	145.9 ± 15.3	147.8 ± 14.9	149.9 ± 15.0	149.9 ± 14.9	148.0 ± 13.6
	KN-HI	431.7 ± 20.4	433.1 ± 20.4	437.6 ± 22.0	441.4 ± 23.6	443.6 ± 23.5	445.1 ± 23.5	446.4 ± 23.7	447.2 ± 23.4	444.9 ± 22.8	439.9 ± 23.3	436.1 ± 22.5	433.4 ± 21.3
	AN-KN	400.4 ± 13.1	402.7 ± 13.1	407.0 ± 12.8	411.5 ± 12.6	414.4 ± 13.0	414.7 ± 16.1	413.9 ± 14.2	413.6 ± 12.8	409.8 ± 12.7	405.7 ± 12.8	401.9 ± 12.9	400.4 ± 12.9
	AN-TO	129.8 ± 8.3	129.3 ± 8.0	130.0 ± 7.9	131.8 ± 7.9	135.8 ± 7.6	140.8 ± 6.7	142.6 ± 7.3	141.3 ± 8.4	138.7 ± 8.9	136.8 ± 9.5	133.1 ± 9.8	131.0 ± 8.8
Left Side	HI-PSIS	147.3 ± 13.8	148.1 ± 13.7	150.3 ± 13.8	151.8 ± 13.7	151.9 ± 13.6	150.0 ± 13.1	148.7 ± 13.0	148.9 ± 12.9	150.6 ± 13.3	152.3 ± 13.8	151.2 ± 14.4	148.8 ± 14.2
	KN-HI	449.3 ± 16.1	449.7 ± 15.8	447.3 ± 15.6	442.5 ± 15.9	438.5 ± 16.0	435.1 ± 15.3	433.0 ± 14.5	434.6 ± 14.5	438.9 ± 14.8	443.5 ± 15.6	446.4 ± 16.1	447.3 ± 16.0
	AN-KN	413.5 ± 11.6	411.8 ± 11.6	408.4 ± 11.6	404.3 ± 11.1	401.2 ± 11.4	399.7 ± 11.8	399.4 ± 11.7	401.3 ± 11.1	405.1 ± 10.8	409.4 ± 11.1	413.3 ± 11.6	413.9 ± 11.9
	AN-TO	141.2 ± 6.1	140.6 ± 7.2	137.7 ± 8.5	135.5 ± 6.8	133.8 ± 7.1	132.9 ± 7.0	131.7 ± 6.7	130.6 ± 6.0	130.8 ± 5.8	132.2 ± 5.7	135.0 ± 6.7	139.0 ± 6.4

TABLE DXII

MEAN SEGMENT LENGTHS AND STANDARD DEVIATION OF SPINE AND TORSO FOR CITY BIKE AT EACH PEDAL ANGLE IN MM

	Pedal Angle [deg.]	0	30	60	90	120	150	180	210	240	270	300	330
Right Side	PSIS-ASIS	175.4 ± 12.1	175.3 ± 12.1	175.4 ± 12.2	175.4 ± 12.6	175.4 ± 12.9	175.1 ± 13.2	174.8 ± 13.3	174.7 ± 13.3	174.4 ± 13.4	174.5 ± 13.3	174.6 ± 12.6	175.1 ± 12.1
	PSIS-L5	56.3 ± 12.0	56.4 ± 12.0	56.3 ± 12.1	56.1 ± 12.0	55.6 ± 12.0	55.4 ± 12.2	55.1 ± 12.2	55.3 ± 12.2	55.7 ± 12.3	55.7 ± 12.1	55.9 ± 12.0	56.1 ± 12.0
	O-TR	149.1 ± 5.8	148.8 ± 6.0	149.0 ± 5.8	149.1 ± 5.8	149.2 ± 6.0	149.3 ± 5.9	149.1 ± 6.0	149.0 ± 6.1	149.0 ± 6.1	149.0 ± 6.1	149.2 ± 5.9	149.0 ± 5.8
	TR-OB	96.4 ± 5.4	96.6 ± 5.2	96.6 ± 5.4	96.6 ± 5.5	96.4 ± 5.4	96.4 ± 5.6	96.4 ± 5.5	96.7 ± 5.7	96.4 ± 5.6	96.3 ± 5.6	96.3 ± 5.5	96.4 ± 5.4
Left Side	PSIS-ASIS	176.3 ± 10.9	176.2 ± 11.0	176.3 ± 11.1	176.3 ± 10.9	176.2 ± 10.3	176.0 ± 9.8	176.4 ± 9.6	176.7 ± 9.8	176.9 ± 9.7	177.0 ± 9.7	177.1 ± 10.1	176.8 ± 10.9
	O-TR	146.1 ± 6.5	146.0 ± 6.0	146.2 ± 6.4	145.9 ± 6.5	145.8 ± 6.6	145.8 ± 6.6	145.8 ± 6.6	145.8 ± 6.6	145.8 ± 6.6	145.8 ± 6.5	145.6 ± 6.6	146.0 ± 6.4
	TR-OB	91.9 ± 5.7	91.8 ± 5.5	91.9 ± 5.5	91.8 ± 5.6	91.7 ± 5.5	91.6 ± 5.4	91.6 ± 5.4	91.6 ± 5.4	91.6 ± 5.4	91.6 ± 5.5	91.6 ± 5.4	91.7 ± 5.3
Torso	PSIS-PSIS	100.5 ± 22.1	100.5 ± 21.9	100.6 ± 21.9	100.7 ± 22.0	100.6 ± 22.0	100.5 ± 22.1	100.5 ± 22.3	100.6 ± 22.3	100.7 ± 22.2	100.6 ± 22.0	100.5 ± 22.0	100.4 ± 22.0
	L5-L3	78.7 ± 13.1	79.5 ± 13.0	79.7 ± 13.0	79.4 ± 12.9	79.3 ± 12.9	78.9 ± 12.6	78.9 ± 13.2	79.7 ± 12.8	79.7 ± 12.9	79.7 ± 13.0	79.7 ± 12.9	79.1 ± 13.1
	L3-T12	103.3 ± 16.7	103.7 ± 16.6	104.1 ± 16.4	104.1 ± 16.6	104.1 ± 16.6	102.6 ± 18.0	103.4 ± 16.7	103.6 ± 16.6	103.1 ± 17.4	104.3 ± 16.5	104.4 ± 16.4	103.4 ± 16.5
	T12-T10	62.2 ± 11.3	62.1 ± 11.5	61.7 ± 11.2	61.5 ± 10.7	61.6 ± 10.6	63.2 ± 10.1	62.6 ± 10.6	62.3 ± 10.6	62.7 ± 10.2	61.8 ± 11.2	61.9 ± 11.3	62.2 ± 11.9
	T10-T7	84.1 ± 7.5	84.0 ± 7.6	84.2 ± 7.6	84.4 ± 7.1	82.4 ± 7.9	84.8 ± 7.4	83.9 ± 7.7	84.1 ± 7.6	81.2 ± 8.8	84.3 ± 7.4	84.5 ± 7.4	84.3 ± 7.6
	T7-T4	84.0 ± 11.6	83.8 ± 11.1	83.9 ± 11.2	84.0 ± 11.3	87.4 ± 11.4	84.1 ± 11.5	84.7 ± 10.9	86.2 ± 11.5	88.4 ± 10.6	86.0 ± 12.0	85.8 ± 12.3	84.1 ± 11.2
	T4-C7	99.2 ± 15.3	99.3 ± 15.7	97.6 ± 16.1	99.0 ± 15.3	97.7 ± 15.2	99.0 ± 15.0	99.1 ± 15.1	96.6 ± 14.2	97.9 ± 15.6	98.1 ± 15.4	96.8 ± 17.4	99.1 ± 15.7
	C7-O	117.0 ± 30.2	117.0 ± 30.5	119.2 ± 29.6	117.0 ± 30.8	117.4 ± 30.9	117.7 ± 31.3	117.2 ± 32.1	118.1 ± 28.2	116.5 ± 30.9	116.6 ± 29.5	117.8 ± 29.5	117.3 ± 30.0

TABLE DXIII

MEAN SEGMENT LENGTHS AND STANDARD DEVIATION OF UPPER EXTREMITIES FOR RACING BIKE AT EACH PEDAL ANGLE IN MM

	Pedal Angle [deg.]	0	30	60	90	120	150	180	210	240	270	300	330
Right Side	SH-C7	240.9 ± 19.0	241.1 ± 18.9	240.8 ± 19.3	240.9 ± 19.5	240.7 ± 19.2	240.6 ± 19.1	240.6 ± 19.0	239.9 ± 18.9	239.3 ± 19.0	238.3 ± 19.5	239.8 ± 19.2	240.4 ± 18.9
	SH-EL	252.2 ± 19.7	252.1 ± 19.6	252.4 ± 19.7	252.9 ± 19.8	253.2 ± 20.0	253.2 ± 20.1	253.1 ± 20.2	253.2 ± 20.0	253.0 ± 19.9	252.8 ± 19.9	252.5 ± 19.8	252.1 ± 19.5
	EL-WR	266.5 ± 8.1	266.5 ± 8.0	266.5 ± 8.1	266.5 ± 8.1	266.3 ± 8.1	266.2 ± 8.1	266.2 ± 8.2	266.4 ± 8.1	266.3 ± 8.1	266.4 ± 8.1	266.5 ± 8.1	266.4 ± 8.2
	WR-FI	72.1 ± 3.9	72.2 ± 3.8	72.2 ± 3.8	72.2 ± 3.8	72.1 ± 3.8	71.9 ± 3.8	71.9 ± 3.7	72.2 ± 3.8	72.1 ± 3.8	72.1 ± 3.7	72.2 ± 3.7	72.1 ± 3.8
	SH-SS	187.9 ± 15.5	187.8 ± 15.4	187.7 ± 15.4	187.7 ± 15.3	187.5 ± 15.2	187.5 ± 15.2	187.5 ± 15.2	187.5 ± 15.1	187.2 ± 15.1	187.5 ± 15.4	187.5 ± 15.4	187.8 ± 15.3
	SH-SI	251.8 ± 15.4	251.8 ± 15.4	251.6 ± 15.4	250.8 ± 15.3	250.5 ± 15.4	250.2 ± 15.2	249.8 ± 15.3	249.7 ± 15.4	249.5 ± 15.5	249.9 ± 15.2	250.2 ± 15.0	251.1 ± 14.8
Left Side	SH-C7	239.4 ± 18.0	238.7 ± 17.9	237.9 ± 18.2	238.0 ± 18.7	237.9 ± 18.9	238.4 ± 18.8	238.9 ± 18.6	239.2 ± 18.1	238.8 ± 18.1	237.9 ± 19.7	239.0 ± 18.5	239.6 ± 18.0
	SH-EL	252.3 ± 21.1	252.6 ± 21.1	252.6 ± 21.0	252.4 ± 20.5	252.3 ± 20.5	251.8 ± 20.2	251.7 ± 20.1	251.5 ± 20.1	251.6 ± 20.1	251.9 ± 20.6	252.1 ± 20.8	252.6 ± 21.1
	EL-WR	266.0 ± 8.0	266.1 ± 8.0	266.1 ± 8.1	266.0 ± 8.2	266.2 ± 8.0	266.2 ± 8.1	266.2 ± 8.1	266.2 ± 8.1	266.2 ± 8.1	266.0 ± 8.3	266.0 ± 8.3	266.0 ± 8.2
	WR-FI	70.2 ± 6.8	70.3 ± 6.9	70.3 ± 6.9	70.3 ± 6.7	70.4 ± 6.7	70.3 ± 6.8	70.4 ± 6.8	70.4 ± 6.8	70.5 ± 6.7	70.4 ± 6.8	70.4 ± 6.8	70.2 ± 6.8
	SH-SS	193.9 ± 22.3	193.8 ± 22.4	193.7 ± 22.8	193.9 ± 23.0	193.9 ± 23.2	194.1 ± 23.3	194.3 ± 23.1	194.3 ± 23.0	194.1 ± 22.7	193.9 ± 22.7	193.8 ± 22.7	193.9 ± 22.4
	SH-SI	242.4 ± 18.6	242.3 ± 18.5	242.2 ± 18.6	242.5 ± 18.5	242.8 ± 18.3	243.2 ± 18.3	243.9 ± 18.6	244.1 ± 18.7	243.6 ± 18.7	243.2 ± 18.8	242.7 ± 18.9	242.6 ± 18.7

TABLE DXIV

MEAN SEGMENT LENGTHS AND STANDARD DEVIATION OF LOWER EXTREMITIES FOR RACING BIKE AT EACH PEDAL ANGLE IN MM

	Pedal Angle [deg.]	0	30	60	90	120	150	180	210	240	270	300	330
Right Side	HI-PSIS	143.2 ± 15.1	142.4 ± 14.6	144.7 ± 15.2	148.8 ± 16.9	150.7 ± 17.4	149.9 ± 17.0	148.4 ± 17.1	148.6 ± 17.0	149.9 ± 17.2	151.1 ± 16.8	150.1 ± 15.9	146.7 ± 15.7
	KN-HI	416.9 ± 22.2	417.7 ± 22.2	423.9 ± 23.5	430.7 ± 24.2	438.1 ± 23.0	443.5 ± 22.8	447.5 ± 23.6	447.8 ± 23.7	444.1 ± 23.1	436.9 ± 23.1	428.6 ± 23.0	422.1 ± 22.3
	AN-KN	416.9 ± 22.2	417.7 ± 22.2	423.9 ± 23.5	430.7 ± 24.2	438.1 ± 23.0	443.5 ± 22.8	447.5 ± 23.6	447.8 ± 23.7	444.1 ± 23.1	436.9 ± 23.1	428.6 ± 23.0	422.1 ± 22.3
	AN-TO	130.1 ± 7.7	129.2 ± 7.5	129.9 ± 7.0	131.2 ± 6.9	134.3 ± 7.4	137.5 ± 7.6	139.6 ± 7.8	140.1 ± 8.0	138.0 ± 8.8	136.9 ± 9.6	134.3 ± 9.4	131.8 ± 8.0
Left Side	HI-PSIS	151.6 ± 17.0	152.0 ± 16.5	152.8 ± 16.4	153.8 ± 16.6	153.0 ± 16.5	149.8 ± 15.2	145.7 ± 14.9	145.3 ± 14.5	148.0 ± 15.1	151.9 ± 16.0	153.8 ± 17.1	152.7 ± 17.5
	KN-HI	450.5 ± 17.2	449.9 ± 16.9	445.4 ± 16.3	438.8 ± 16.6	431.7 ± 16.9	424.4 ± 17.0	419.7 ± 16.5	420.2 ± 16.4	425.7 ± 16.3	434.1 ± 17.3	441.4 ± 17.9	447.3 ± 18.1
	AN-KN	413.0 ± 10.8	409.4 ± 11.8	405.6 ± 11.2	402.7 ± 11.2	400.2 ± 10.8	398.5 ± 10.9	398.7 ± 10.8	400.6 ± 10.6	403.9 ± 10.4	408.0 ± 11.1	412.0 ± 11.5	413.4 ± 11.5
	AN-TO	145.1 ± 20.3	146.2 ± 21.1	144.6 ± 21.1	142.4 ± 21.3	139.2 ± 21.1	137.9 ± 20.9	135.8 ± 20.8	135.2 ± 21.0	135.8 ± 21.3	137.6 ± 20.7	140.6 ± 20.8	143.3 ± 20.5

TABLE DXV
MEAN SEGMENT LENGTHS AND STANDARD DEVIATION OF SPINE AND TORSO FOR RACING BIKE AT EACH PEDAL ANGLE IN MM

	Pedal Angle [deg.]	0	30	60	90	120	150	180	210	240	270	300	330
Right Side	PSIS-ASIS	172.9 ± 11.2	172.1 ± 11.0	172.6 ± 11.0	174.0 ± 12.0	174.6 ± 13.1	175.3 ± 13.4	175.2 ± 14.5	175.5 ± 14.2	175.5 ± 14.0	175.4 ± 13.5	175.1 ± 13.1	173.8 ± 11.8
	PSIS-L5	55.7 ± 12.1	55.7 ± 12.2	55.9 ± 12.2	56.0 ± 12.2	55.8 ± 12.4	55.6 ± 12.4	55.4 ± 12.4	55.3 ± 12.4	55.5 ± 12.4	55.6 ± 12.3	55.8 ± 12.1	55.8 ± 12.2
	O-TR	151.1 ± 5.4	151.1 ± 5.4	151.1 ± 5.4	151.0 ± 5.3	151.0 ± 5.2	151.0 ± 5.2	151.1 ± 5.3	151.1 ± 5.3	151.1 ± 5.4	151.1 ± 5.3	151.0 ± 5.3	151.1 ± 5.2
	TR-OB	96.4 ± 5.6	96.5 ± 5.6	96.4 ± 5.5	96.5 ± 5.6	96.5 ± 5.7	96.4 ± 5.7	96.6 ± 5.7	96.6 ± 5.7	96.3 ± 5.6	96.4 ± 5.6	96.5 ± 5.7	96.6 ± 5.7
Left Side	PSIS-ASIS	178.4 ± 11.6	178.1 ± 11.1	177.6 ± 10.3	177.5 ± 10.2	176.6 ± 9.8	175.9 ± 9.0	174.2 ± 9.6	173.8 ± 10.4	174.4 ± 10.6	176.2 ± 10.7	177.3 ± 11.1	178.1 ± 11.6
	O-TR	149.7 ± 5.9	149.6 ± 5.9	149.7 ± 5.8	149.7 ± 5.8	149.6 ± 5.8	149.7 ± 5.8	149.8 ± 5.9	149.8 ± 5.9	149.7 ± 6.0	149.7 ± 5.9	149.7 ± 5.9	149.6 ± 5.9
	TR-OB	91.9 ± 6.0	91.9 ± 6.0	91.9 ± 5.9	91.8 ± 5.9	91.7 ± 5.9	91.7 ± 5.9	91.7 ± 5.9	91.8 ± 5.8	91.8 ± 5.8	91.8 ± 5.9	91.9 ± 5.9	91.8 ± 6.0
Torso	PSIS-PSIS	100.6 ± 22.3	100.6 ± 22.2	100.8 ± 22.2	101.1 ± 22.3	101.2 ± 22.3	101.1 ± 22.3	100.7 ± 22.2	100.8 ± 22.1	101.1 ± 22.0	101.1 ± 22.2	101.1 ± 22.3	100.8 ± 22.3
	L5-L3	85.8 ± 13.9	86.0 ± 14.0	85.9 ± 14.0	85.7 ± 13.9	85.7 ± 13.5	85.6 ± 13.5	85.7 ± 13.5	85.9 ± 13.5	86.0 ± 13.6	86.0 ± 13.6	85.9 ± 13.8	85.7 ± 13.8
	L3-T12	108.8 ± 18.3	108.9 ± 18.3	108.8 ± 18.2	108.6 ± 18.1	108.7 ± 18.2	108.7 ± 18.2	108.8 ± 18.2	108.9 ± 18.3	108.8 ± 18.2	108.8 ± 18.3	108.8 ± 18.3	108.8 ± 18.3
	T12-T10	63.3 ± 8.2	63.3 ± 8.2	63.2 ± 8.2	63.0 ± 8.3	63.2 ± 8.4	63.3 ± 8.4	63.4 ± 8.4	63.4 ± 8.4	63.3 ± 8.3	63.1 ± 8.3	63.1 ± 8.3	63.2 ± 8.3
	T10-T7	85.2 ± 7.0	85.2 ± 7.0	85.1 ± 6.9	84.9 ± 6.9	85.0 ± 6.8	85.0 ± 6.8	85.1 ± 6.8	85.1 ± 7.0	84.9 ± 7.1	84.9 ± 6.9	84.9 ± 6.9	85.2 ± 6.9
	T7-T4	86.3 ± 10.5	85.7 ± 10.9	85.7 ± 10.8	85.6 ± 10.8	85.6 ± 10.7	85.6 ± 10.7	85.5 ± 10.7	85.6 ± 10.8	85.5 ± 10.9	85.6 ± 10.8	85.5 ± 10.8	86.2 ± 10.6
	T4-C7	93.1 ± 15.1	93.2 ± 15.1	93.2 ± 15.1	93.1 ± 15.0	93.1 ± 15.0	93.1 ± 15.1	93.1 ± 15.0	93.0 ± 15.1	93.0 ± 15.1	93.3 ± 14.8	93.1 ± 15.0	93.2 ± 15.0
	C7-O	100.2 ± 35.0	100.2 ± 35.0	100.5 ± 35.2	100.4 ± 35.4	100.4 ± 35.5	100.6 ± 35.7	100.8 ± 36.0	101.3 ± 36.0	101.6 ± 36.2	101.4 ± 36.4	100.9 ± 35.5	100.1 ± 34.9

TABLE DXIII

MEAN SEGMENT LENGTHS AND STANDARD DEVIATION OF UPPER EXTREMITIES FOR MOUNTAIN BIKE AT EACH PEDAL ANGLE IN MM

	Pedal Angle [deg.]	0	30	60	90	120	150	180	210	240	270	300	330
Right Side	SH-C7	219.2 ± 30.4	219.7 ± 30.2	219.3 ± 30.3	218.9 ± 30.3	218.7 ± 30.5	218.7 ± 30.6	218.6 ± 30.8	217.9 ± 30.8	217.8 ± 30.7	218.3 ± 30.5	218.6 ± 30.4	218.8 ± 30.5
	SH-EL	259.7 ± 20.0	259.6 ± 20.1	259.8 ± 20.1	260.1 ± 20.2	260.4 ± 20.5	260.6 ± 20.6	260.6 ± 20.7	260.9 ± 20.5	260.8 ± 20.4	260.6 ± 20.4	260.3 ± 20.2	260.1 ± 20.1
	EL-WR	263.4 ± 8.6	263.4 ± 8.6	263.4 ± 8.6	263.3 ± 8.7	263.4 ± 8.6	263.4 ± 8.6	263.4 ± 8.6	263.3 ± 8.7	263.3 ± 8.7	263.5 ± 8.6	263.4 ± 8.6	263.4 ± 8.6
	WR-FI	83.3 ± 5.4	83.5 ± 5.4	83.4 ± 5.4	83.2 ± 5.4	83.1 ± 5.3	82.9 ± 5.2	82.9 ± 5.3	82.7 ± 5.2	82.9 ± 5.3	82.9 ± 5.3	83.0 ± 5.3	83.1 ± 5.3
	SH-SS	171.3 ± 15.6	171.3 ± 15.7	171.1 ± 15.7	170.8 ± 15.6	170.5 ± 15.7	170.4 ± 15.7	170.3 ± 15.7	170.1 ± 15.8	170.0 ± 15.8	170.3 ± 15.8	170.6 ± 15.8	171.0 ± 15.6
	SH-SI	227.6 ± 16.7	227.6 ± 16.9	227.1 ± 17.1	226.5 ± 17.0	226.1 ± 17.1	225.8 ± 17.1	225.5 ± 17.2	225.4 ± 17.1	225.3 ± 17.2	225.6 ± 17.2	226.1 ± 16.9	226.9 ± 16.6
Left Side	SH-C7	218.4 ± 28.5	217.9 ± 28.6	217.5 ± 29.1	217.5 ± 29.1	217.6 ± 29.1	217.7 ± 29.4	218.2 ± 29.1	218.5 ± 29.0	218.3 ± 28.7	218.2 ± 28.8	218.2 ± 29.0	218.3 ± 28.9
	SH-EL	260.5 ± 23.1	260.7 ± 23.2	260.7 ± 23.2	260.5 ± 23.1	260.5 ± 23.1	260.2 ± 22.9	259.8 ± 22.8	259.8 ± 22.9	259.7 ± 22.8	260.0 ± 22.8	260.2 ± 22.9	260.6 ± 23.2
	EL-WR	263.0 ± 8.9	263.0 ± 8.8	263.0 ± 8.9	262.9 ± 8.8	263.0 ± 8.9	263.0 ± 8.9	263.1 ± 8.9	263.1 ± 8.9	263.0 ± 8.8	263.1 ± 8.9	263.0 ± 8.9	263.0 ± 8.9
	WR-FI	78.5 ± 7.0	78.5 ± 7.0	78.6 ± 7.0	78.6 ± 7.0	78.7 ± 7.1	78.8 ± 7.1	79.2 ± 7.1	79.2 ± 7.1	79.0 ± 7.0	78.8 ± 7.0	78.7 ± 7.0	78.6 ± 6.9
	SH-SS	171.9 ± 16.7	171.8 ± 16.6	171.6 ± 16.8	171.6 ± 16.7	171.6 ± 16.6	171.6 ± 16.8	171.9 ± 16.6	172.0 ± 16.6	172.1 ± 16.4	172.1 ± 16.6	172.1 ± 16.7	171.8 ± 16.6
	SH-SI	223.7 ± 9.5	223.5 ± 9.6	223.4 ± 9.8	223.6 ± 9.8	224.0 ± 9.9	224.3 ± 10.3	224.8 ± 10.5	225.0 ± 10.5	224.8 ± 10.3	224.6 ± 10.4	224.4 ± 10.0	224.0 ± 9.8

TABLE DXIV

MEAN SEGMENT LENGTHS AND STANDARD DEVIATION OF LOWER EXTREMITIES FOR MOUNTAIN BIKE AT EACH PEDAL ANGLE IN MM

	Pedal Angle [deg.]	0	30	60	90	120	150	180	210	240	270	300	330
Right Side	HI-PSIS	141.3 ± 12.8	141.0 ± 12.3	143.8 ± 14.1	147.4 ± 15.9	148.4 ± 16.0	147.2 ± 14.6	145.2 ± 14.5	145.9 ± 14.2	147.4 ± 13.8	149.7 ± 13.3	147.8 ± 13.6	144.3 ± 13.0
	KN-HI	422.0 ± 20.3	423.4 ± 20.1	428.4 ± 21.4	435.1 ± 22.4	441.6 ± 22.6	447.3 ± 21.7	449.3 ± 21.8	448.5 ± 22.0	445.3 ± 21.6	438.1 ± 21.3	431.3 ± 21.6	425.7 ± 21.2
	AN-KN	398.3 ± 13.3	400.4 ± 13.6	404.4 ± 13.6	408.6 ± 14.0	412.6 ± 13.8	413.9 ± 13.6	412.2 ± 12.8	409.6 ± 12.5	407.1 ± 13.8	402.0 ± 12.2	399.9 ± 12.8	398.2 ± 13.0
	AN-TO	129.4 ± 7.9	128.5 ± 7.3	129.1 ± 7.5	130.4 ± 7.9	133.2 ± 8.3	135.9 ± 8.8	138.1 ± 9.4	137.1 ± 9.3	135.5 ± 9.7	133.9 ± 9.4	132.0 ± 9.1	130.3 ± 7.8
Left Side	HI-PSIS	147.3 ± 13.7	147.4 ± 13.4	148.6 ± 13.6	149.7 ± 13.8	148.5 ± 13.9	144.7 ± 12.1	141.9 ± 11.1	142.6 ± 10.9	145.6 ± 11.4	149.1 ± 12.4	150.1 ± 13.5	148.7 ± 13.5
	KN-HI	453.6 ± 14.7	453.1 ± 14.8	449.2 ± 14.7	442.4 ± 15.3	434.9 ± 15.6	428.9 ± 14.6	425.5 ± 13.4	426.7 ± 12.7	432.5 ± 12.9	439.7 ± 13.4	445.9 ± 13.5	450.5 ± 14.1
	AN-KN	411.4 ± 10.8	408.6 ± 10.2	406.0 ± 10.5	404.0 ± 10.5	400.2 ± 9.9	398.2 ± 10.3	398.4 ± 10.6	400.4 ± 10.1	403.6 ± 10.2	407.3 ± 10.6	412.5 ± 12.6	411.9 ± 11.6
	AN-TO	138.4 ± 7.7	137.8 ± 7.4	136.2 ± 7.6	133.4 ± 7.5	132.5 ± 7.3	131.4 ± 6.1	130.4 ± 6.5	130.1 ± 6.1	130.7 ± 6.0	132.1 ± 5.8	134.7 ± 7.2	136.5 ± 6.8

TABLE DXV

MEAN SEGMENT LENGTHS AND STANDARD DEVIATION OF SPINE AND TORSO FOR MOUNTAIN BIKE AT EACH PEDAL ANGLE IN MM

	Pedal Angle [deg.]	0	30	60	90	120	150	180	210	240	270	300	330
Right Side	PSIS-ASIS	173.7 ± 12.1	173.4 ± 12.0	173.4 ± 12.5	173.5 ± 13.2	173.7 ± 13.7	174.2 ± 13.5	173.7 ± 13.7	173.7 ± 13.8	173.8 ± 13.8	175.1 ± 12.8	174.3 ± 13.0	174.0 ± 12.4
	PSIS-L5	55.8 ± 12.2	56.0 ± 12.2	56.0 ± 12.3	56.1 ± 12.4	56.0 ± 12.4	55.3 ± 12.2	55.7 ± 12.3	55.7 ± 12.3	55.6 ± 12.4	54.9 ± 12.1	55.9 ± 12.3	55.9 ± 12.4
	O-TR	150.0 ± 5.8	150.0 ± 5.8	150.0 ± 5.8	150.0 ± 5.7	149.8 ± 5.8	149.9 ± 5.8	149.8 ± 5.7	149.9 ± 5.8	149.8 ± 5.7	149.9 ± 5.8	149.8 ± 5.9	149.7 ± 5.9
	TR-OB	96.5 ± 5.6	96.5 ± 5.5	96.5 ± 5.6	96.5 ± 5.7	96.4 ± 5.6	96.4 ± 5.5	96.4 ± 5.4	96.4 ± 5.4	96.3 ± 5.3	96.4 ± 5.5	96.4 ± 5.4	96.4 ± 5.5
Left Side	PSIS-ASIS	176.9 ± 10.8	176.7 ± 10.8	176.4 ± 10.7	176.1 ± 10.3	175.7 ± 9.7	174.8 ± 8.4	174.5 ± 8.0	174.4 ± 8.1	175.1 ± 8.6	176.2 ± 9.7	176.9 ± 10.5	177.3 ± 10.9
	O-TR	147.6 ± 6.4	147.7 ± 6.3	147.7 ± 6.3	147.7 ± 6.3	147.7 ± 6.2	147.7 ± 6.3	147.8 ± 6.3	147.8 ± 6.3	147.9 ± 6.2	147.8 ± 6.3	147.7 ± 6.3	147.8 ± 6.3
	TR-OB	91.5 ± 5.9	91.5 ± 6.0	91.5 ± 6.0	91.5 ± 5.9	91.5 ± 5.8	91.4 ± 5.9	91.3 ± 6.0	91.3 ± 6.0	91.5 ± 6.0	91.5 ± 5.8	91.5 ± 6.0	91.4 ± 5.9
Torso	PSIS-PSIS	100.7 ± 22.4	100.7 ± 22.2	100.7 ± 22.4	100.9 ± 22.5	101.0 ± 22.5	100.3 ± 22.2	100.5 ± 22.6	100.5 ± 22.6	100.8 ± 22.6	100.1 ± 22.0	101.1 ± 22.6	101.0 ± 22.7
	L5-L3	84.2 ± 13.4	84.4 ± 13.5	84.3 ± 13.3	84.5 ± 12.8	84.2 ± 13.2	84.5 ± 12.8	84.7 ± 13.0	85.3 ± 12.9	85.5 ± 12.5	84.6 ± 13.2	84.4 ± 13.3	84.0 ± 13.3
	L3-T12	104.9 ± 16.7	105.0 ± 16.6	105.1 ± 16.6	105.0 ± 16.7	105.0 ± 16.6	105.0 ± 16.6	105.0 ± 16.6	105.1 ± 16.4	105.1 ± 16.4	105.0 ± 16.4	104.9 ± 16.5	104.8 ± 16.6
	T12-T10	63.5 ± 10.6	63.6 ± 10.8	63.5 ± 10.5	63.3 ± 10.2	63.3 ± 10.2	63.3 ± 10.4	63.5 ± 10.9	63.7 ± 11.2	63.6 ± 10.9	63.5 ± 10.7	63.5 ± 10.9	63.5 ± 10.8
	T10-T7	85.5 ± 6.6	85.4 ± 6.7	85.3 ± 6.7	85.2 ± 6.8	85.3 ± 6.8	85.3 ± 6.8	85.3 ± 6.7	85.2 ± 6.7	85.2 ± 6.7	85.2 ± 6.7	85.3 ± 6.7	85.4 ± 6.7
	T7-T4	83.5 ± 11.5	83.5 ± 11.5	83.6 ± 11.6	83.7 ± 11.5	83.7 ± 11.5	83.6 ± 11.4	83.3 ± 11.5	83.3 ± 11.6	83.3 ± 11.7	83.4 ± 11.6	83.5 ± 11.6	83.5 ± 11.5
	T4-C7	97.1 ± 14.1	97.0 ± 14.0	97.2 ± 13.8	97.2 ± 14.0	97.2 ± 14.0	97.1 ± 14.1	97.2 ± 14.3	97.1 ± 14.3	96.9 ± 14.2	97.1 ± 14.2	97.2 ± 14.1	97.0 ± 14.2
	C7-O	110.2 ± 29.7	110.2 ± 29.9	110.1 ± 30.0	110.4 ± 30.2	110.4 ± 30.1	110.6 ± 30.3	110.7 ± 30.9	110.7 ± 31.2	111.2 ± 31.4	111.5 ± 31.6	111.3 ± 31.8	111.5 ± 31.9

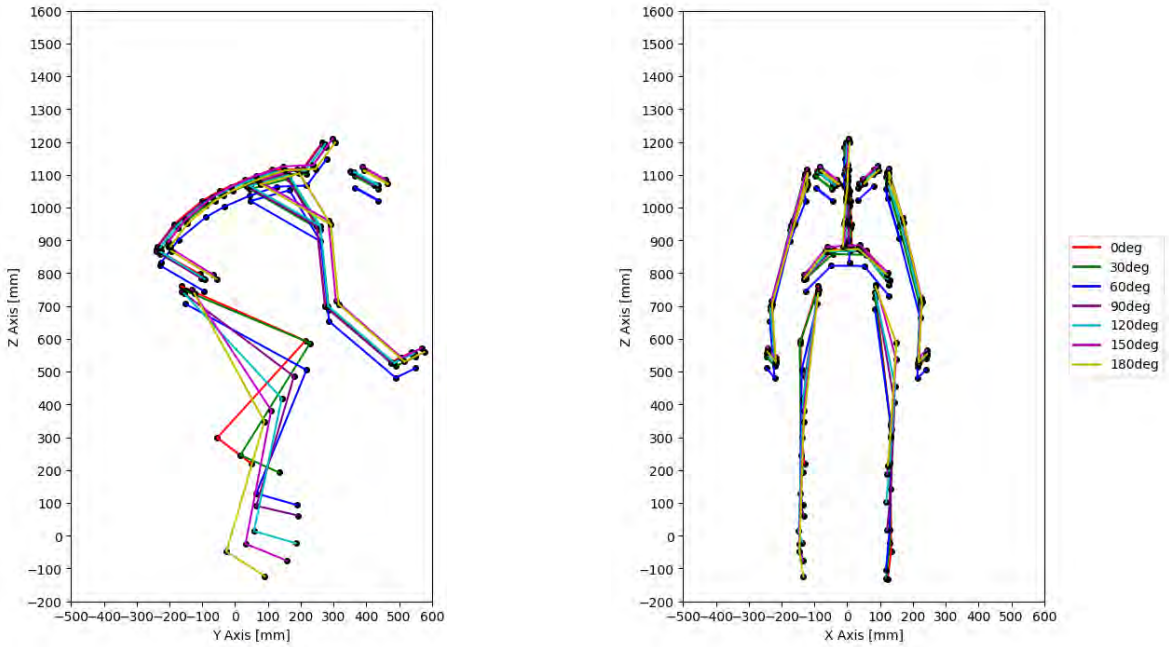

Fig. D1. Kinematic linkage models created from the mean characteristic angles and mean segment lengths of participants riding the racing bike at pedal angles from 0° to 180°, with 30° increments.

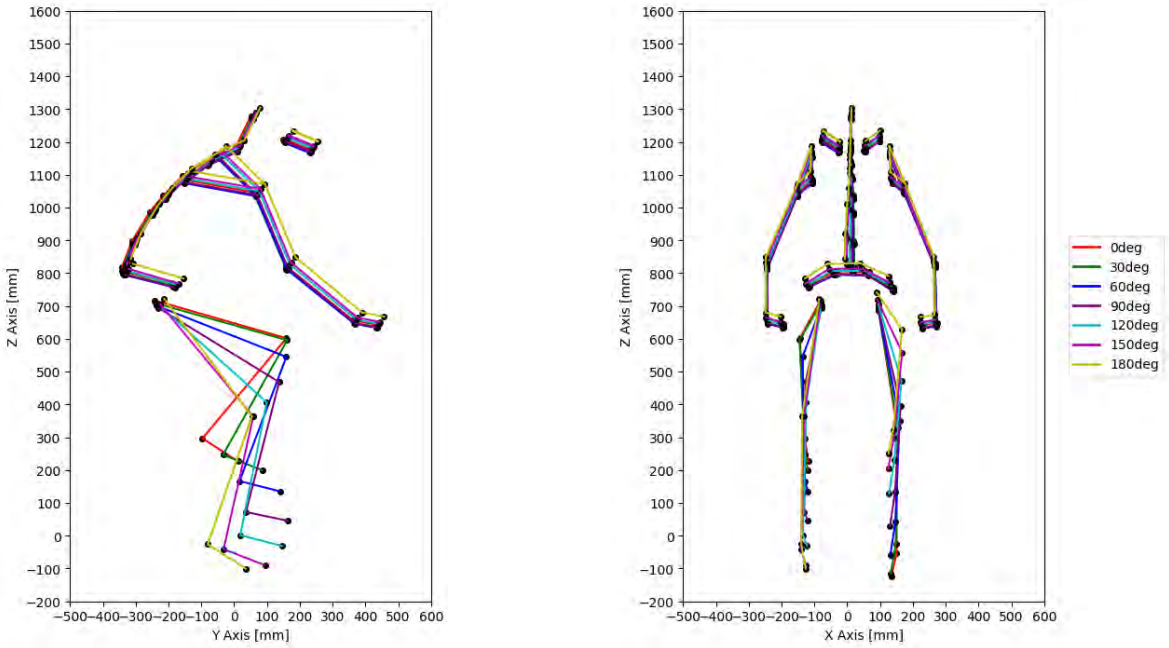

Fig. D2. Kinematic linkage models created from the mean characteristic angles and mean segment lengths of participants riding the mountain bike at pedal angles from 0° to 180°, with 30° increments.

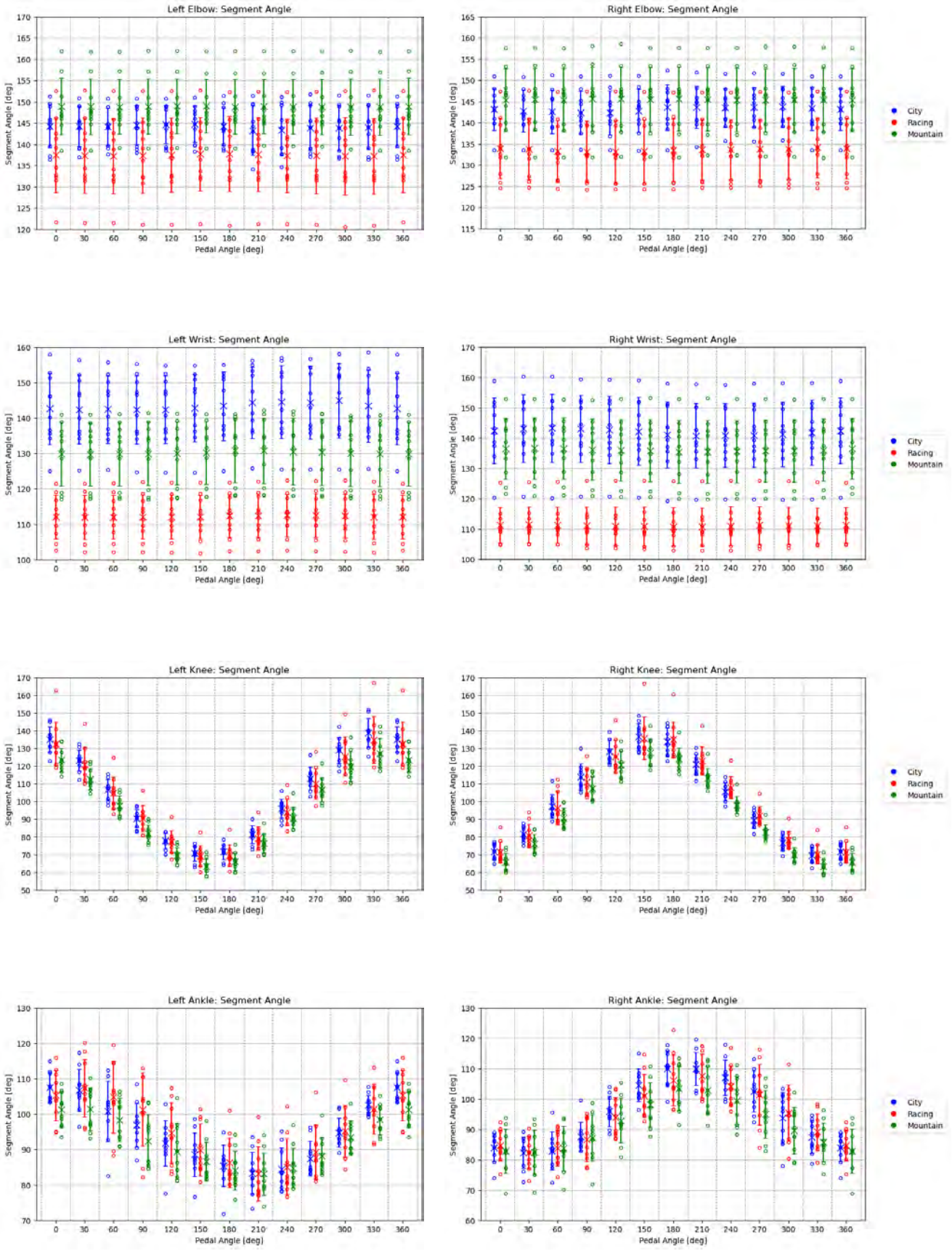

Fig. D3. Mean left and right elbow, wrist, knee, and ankle segment angles for city, racing, and mountain bikes at each pedal angle.

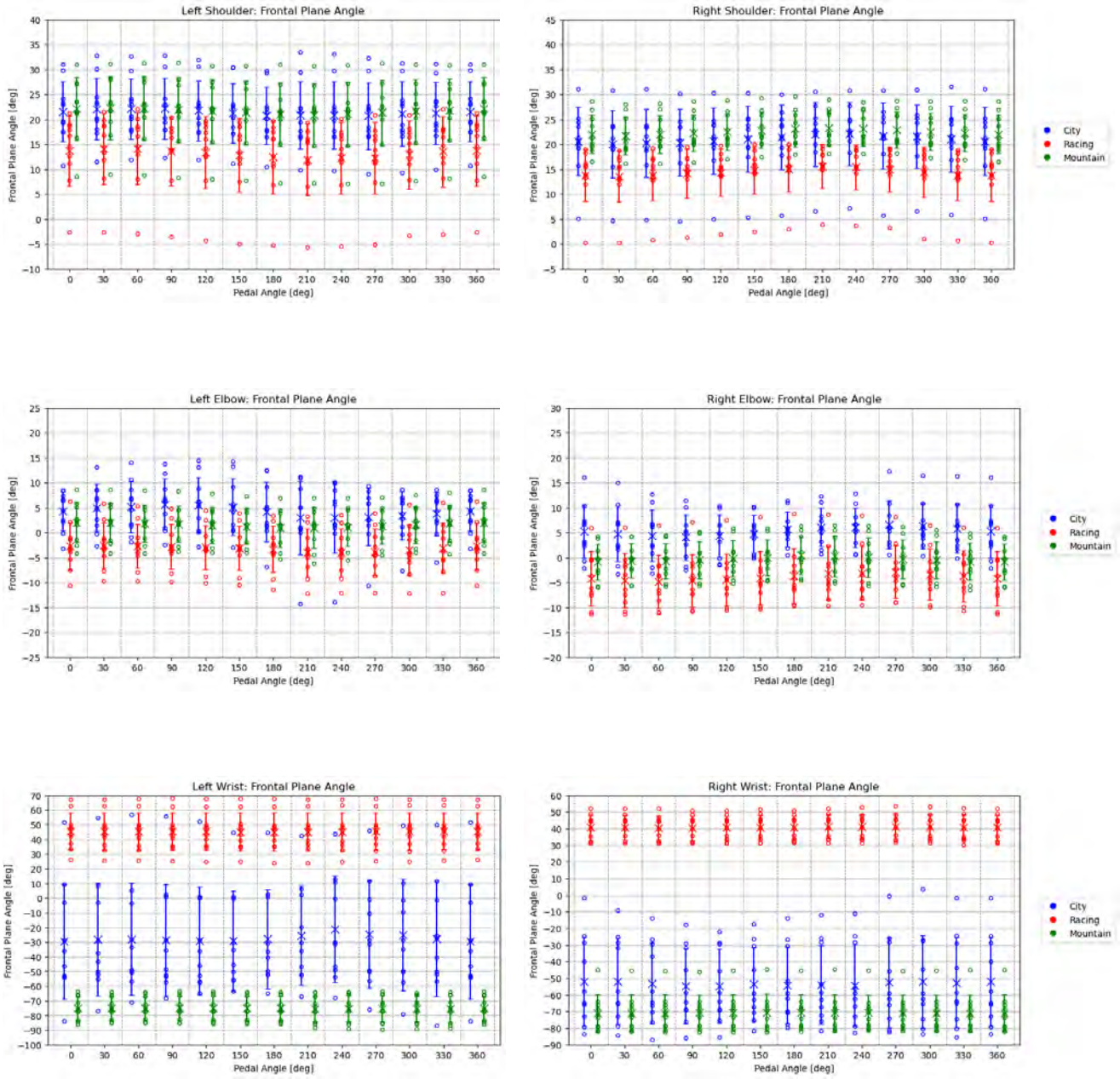

Fig. D4. Mean left and right shoulder, elbow, and wrist angles in frontal plane for city, racing, and mountain bikes at each pedal angle.

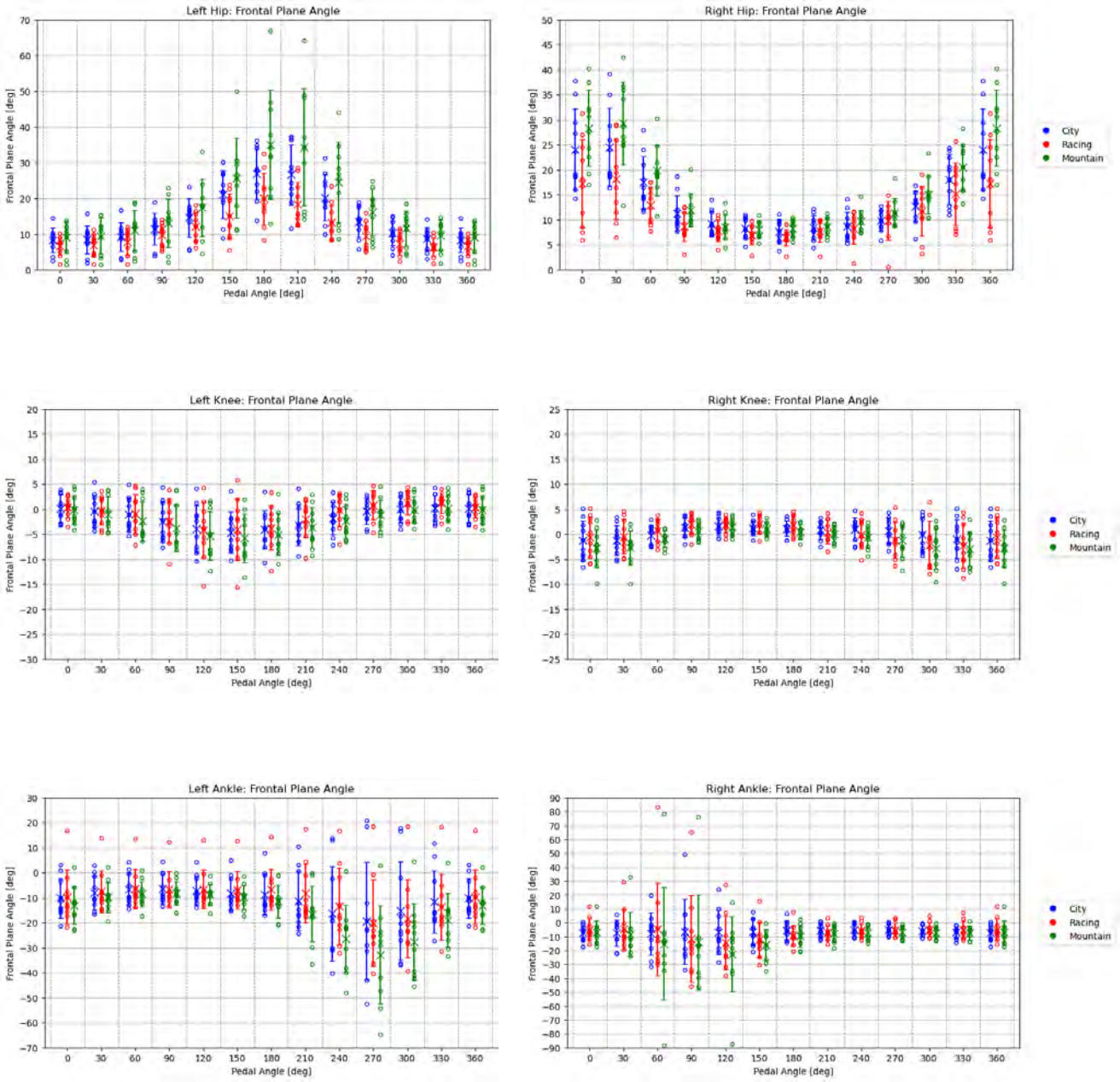

Fig. D5. Mean left and right hip, knee, and ankle angles in frontal plane for city, racing, and mountain bikes at each pedal angle.

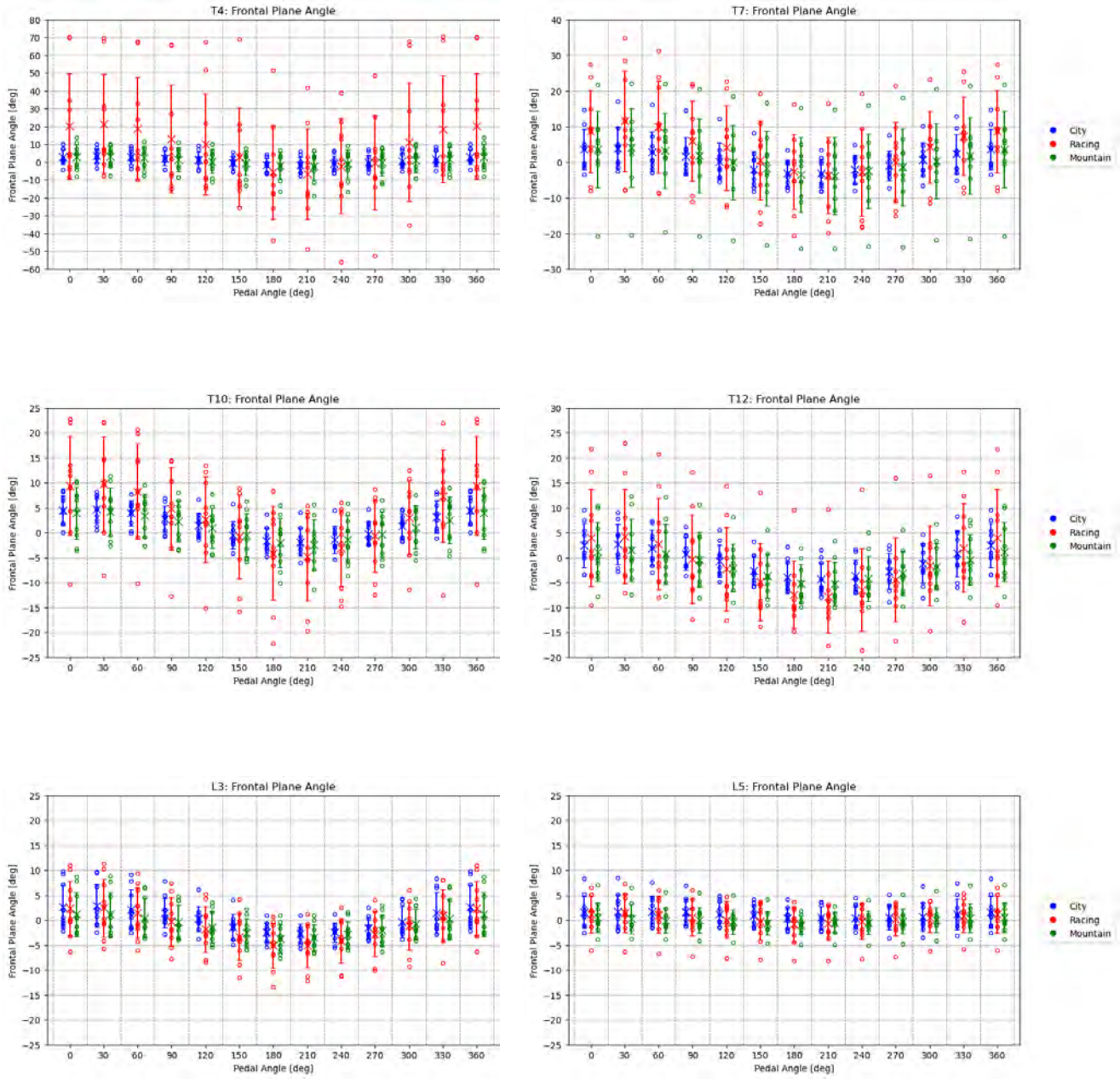

Fig. D6. Mean T4, T7, T10, T12, L3, and L5 vertebrae angles in frontal plane for city, racing, and mountain bikes at each pedal angle.

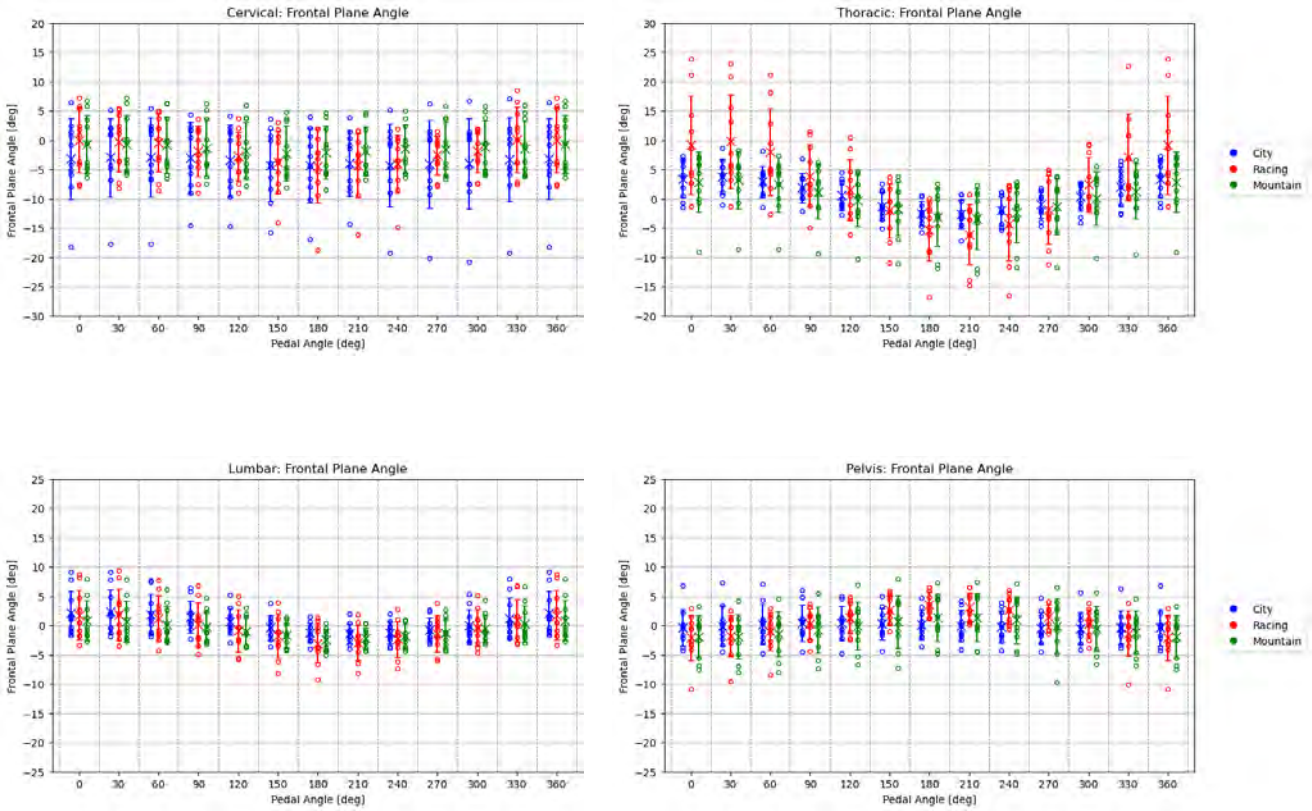

Fig. D7. Mean cervical, thoracic, lumbar, and pelvis angles in frontal plane for city, racing, and mountain bikes at each pedal angle.

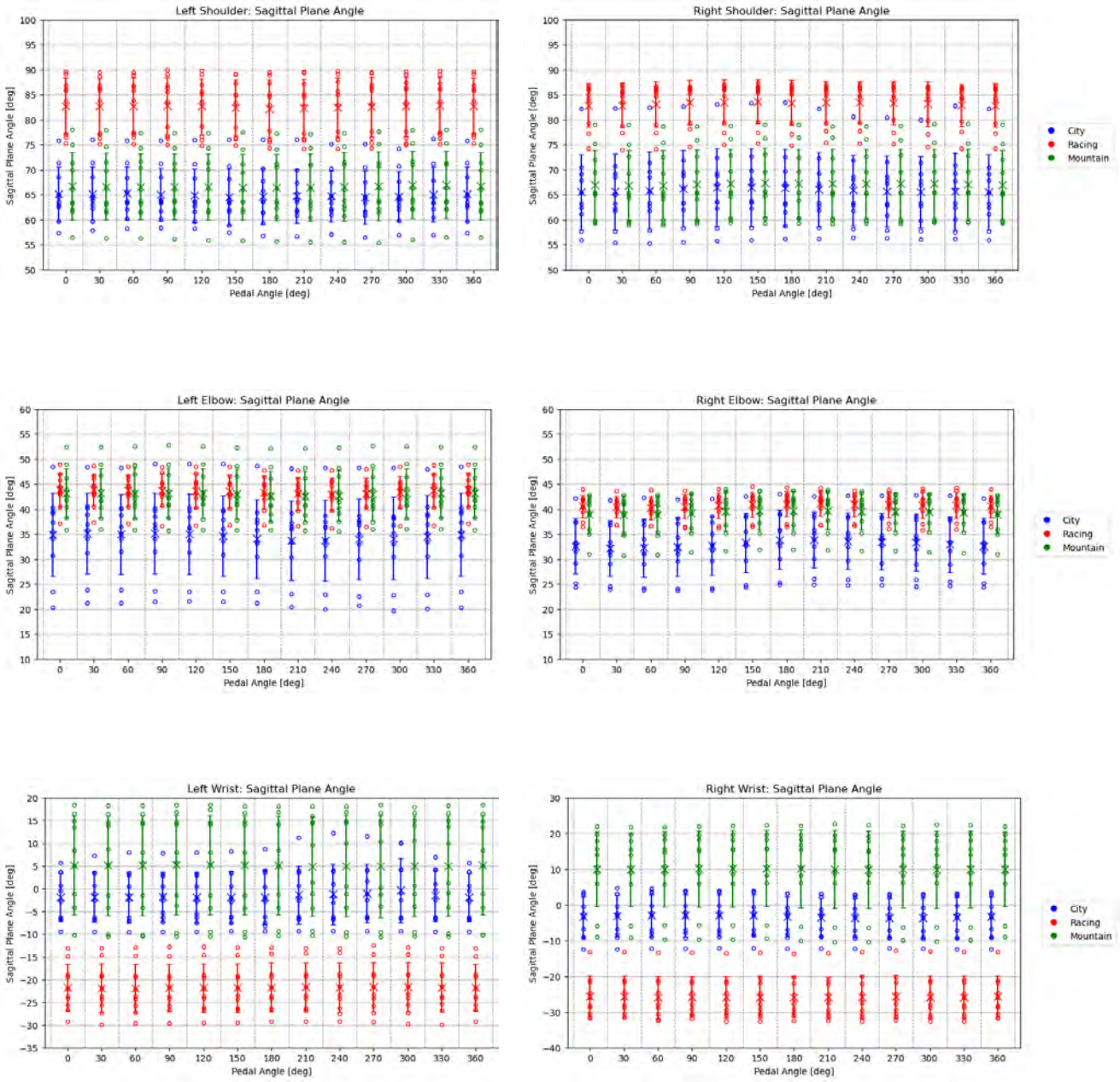

Fig. D8. Mean left and right shoulder, elbow, and wrist angles in sagittal plane for city, racing, and mountain bikes at each pedal angle.

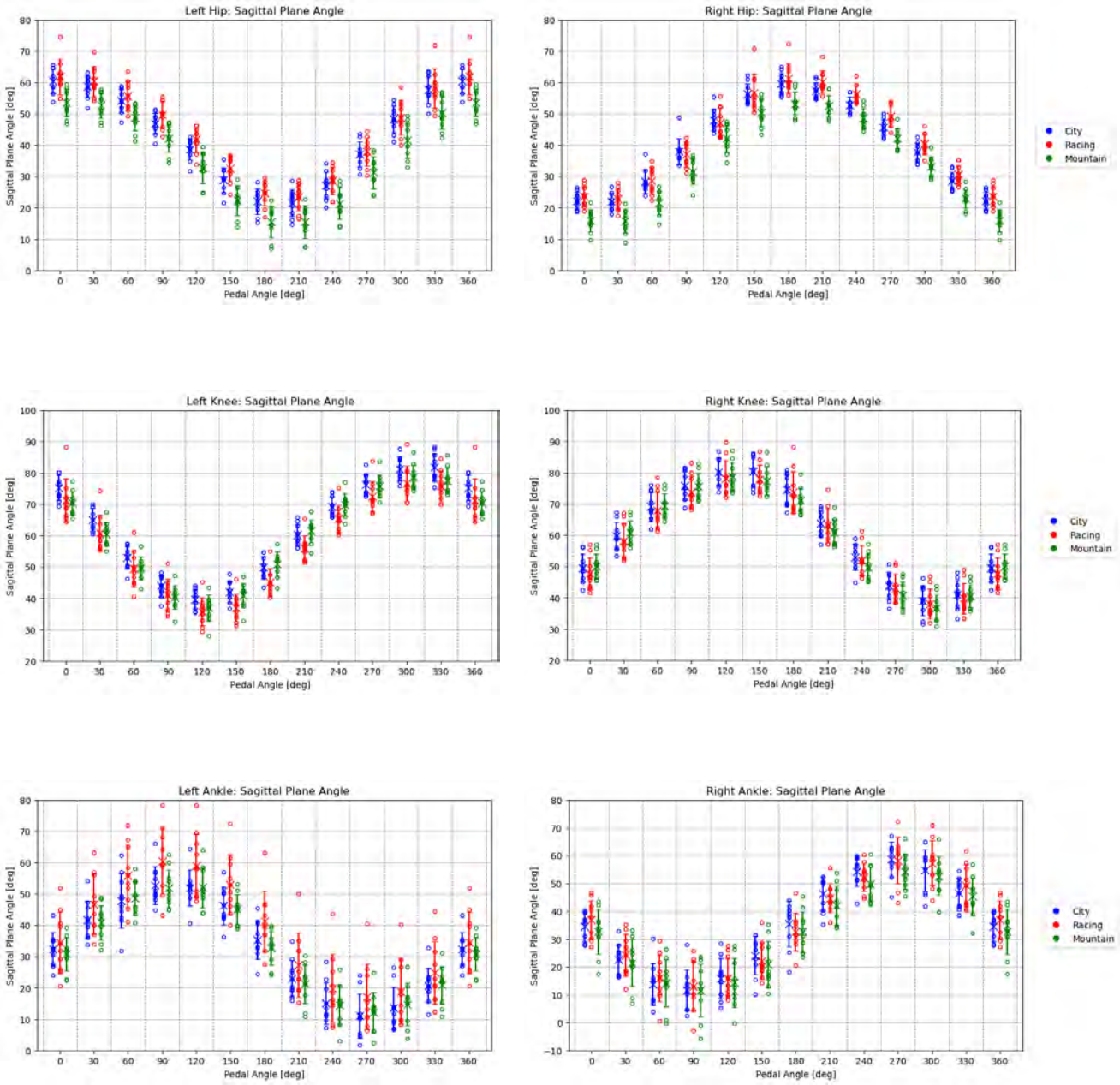

Fig. D9. Mean left and right hip, knee, and ankle angles in sagittal plane for city, racing, and mountain bikes at each pedal angle.

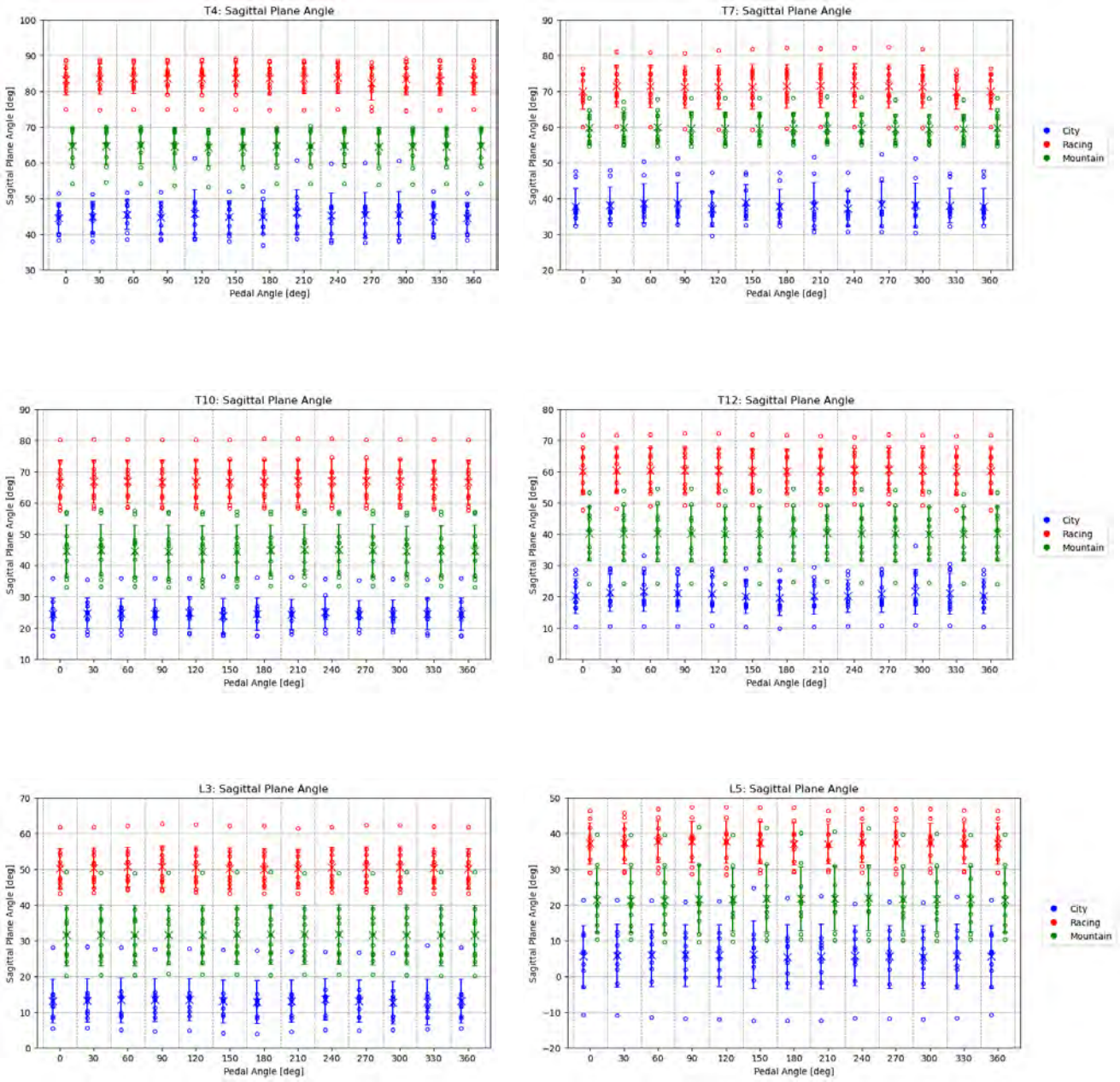

Fig. D10. Mean T4, T7, T10, T12, L3, and L5 vertebrae angles in sagittal plane for city, racing, and mountain bikes at each pedal angle.

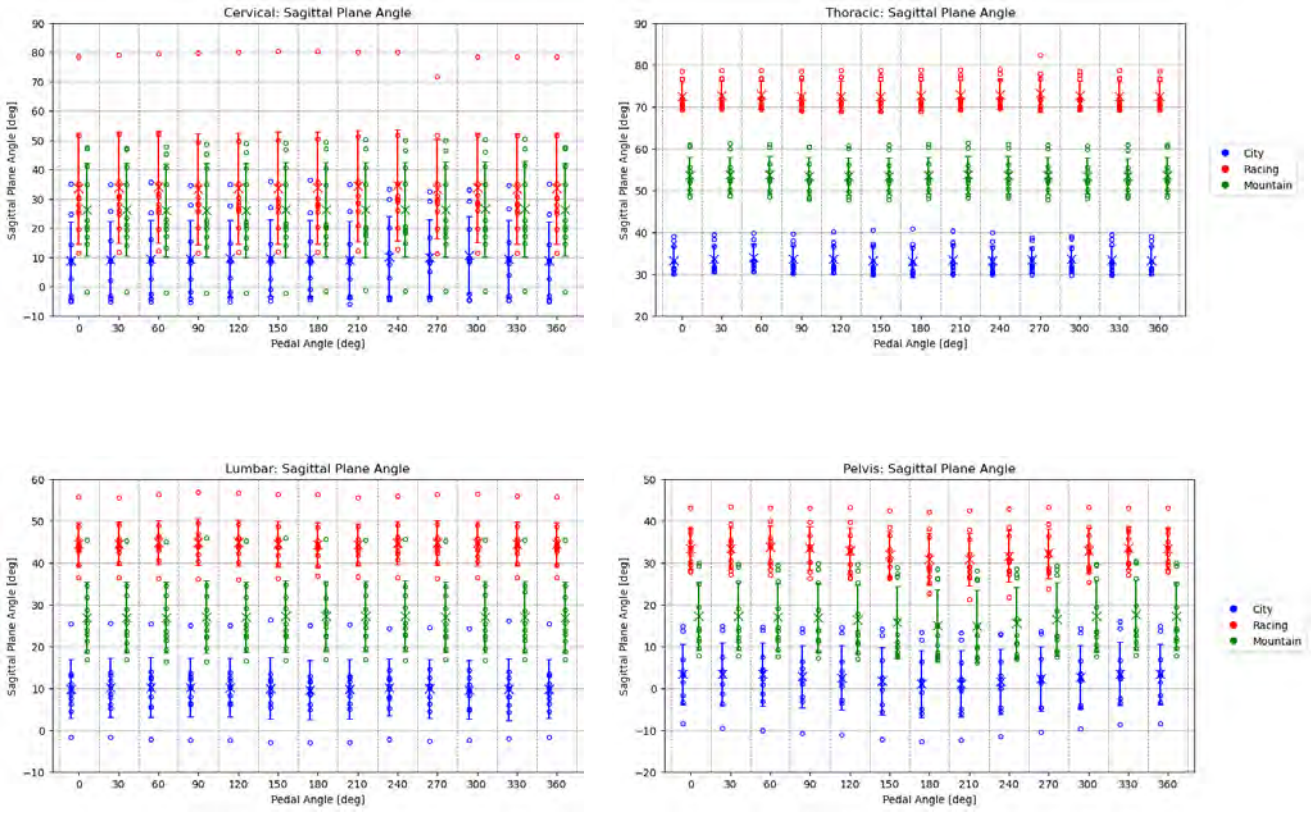

Fig. D11. Mean cervical, thoracic, lumbar, and pelvis angles in sagittal plane for city, racing, and mountain bikes at each pedal angle.

TABLE DXVI
COEFFICIENTS OF THE SINE WAVE FITTED TO MEAN CHARACTERISTIC ANGLES FOR EACH BIKE.
SINE WAVE FORMULA: ASIN(BX+C)+D

			City				Racing				Mountain			
			A	B	C	D	A	B	C	D	A	B	C	D
Right Side	Hip	Front.	19.90	0.01	3.17	26.77	8.02	0.01	2.65	14.39	27.81	0.01	3.28	34.70
		Sag.	19.09	0.02	-1.62	40.39	19.54	0.02	-1.76	42.14	19.77	0.02	-1.62	34.54
	Knee	Front.	2.59	0.01	-0.07	-1.18	2.04	0.02	-0.73	0.21	2.17	0.02	-1.05	-0.93
		Sag.	20.67	0.02	-0.63	60.87	20.26	0.02	-0.64	59.41	20.61	0.02	-0.51	59.32
		Segm.	33.02	0.02	-1.21	102.3	32.61	0.02	-1.27	102.4	31.73	0.02	-1.17	95.06
	Ankle	Front.	-1.14	0.02	0.77	-6.42	-4.11	0.02	-1.23	-7.81	-6.02	0.02	-0.61	-10.81
		Sag.	-23.05	0.02	0.04	34.90	-22.69	0.02	-0.05	35.24	-21.39	0.02	0.00	32.62
		Segm.	14.34	0.02	-2.19	96.23	-12.39	0.02	0.96	94.86	10.34	0.02	-2.11	92.39
Left Side	Hip	Front.	9.04	0.02	-2.43	16.20	6.03	0.02	-2.32	11.94	12.26	0.02	-2.46	19.82
		Sag.	19.40	0.02	1.20	41.22	18.90	0.02	1.16	43.19	19.24	0.02	1.12	34.82
	Knee	Front.	2.38	0.02	1.73	-2.01	-2.68	0.02	-1.06	-1.35	-2.89	0.02	-1.11	-2.63
		Sag.	-21.07	0.02	-0.65	61.62	-20.78	0.02	-0.68	57.26	-20.78	0.02	-0.53	59.45
		Segm.	34.02	0.02	2.01	103.6	33.08	0.02	1.98	101.5	31.54	0.02	2.01	94.84
	Ankle	Front.	5.30	0.02	-0.08	-10.74	5.70	0.02	-0.19	-10.25	10.70	0.02	-0.03	-15.78
		Sag.	21.02	0.02	-0.10	32.76	22.40	0.02	-0.15	38.17	20.65	0.02	-0.09	32.14
		Segm.	12.47	0.02	1.64	95.82	11.60	0.02	1.06	95.37	9.41	0.02	1.55	92.55
Torso	T4	Front.	2.35	0.02	1.02	0.90	13.75	0.02	0.97	7.98	2.48	0.02	1.21	0.68
	T7	Front.	3.51	0.02	1.23	0.36	6.93	0.02	0.97	3.39	3.76	0.02	1.19	0.22
	T10	Front.	3.31	0.02	1.14	1.41	7.21	0.02	1.16	2.71	3.15	0.02	1.17	1.03
	T12	Front.	3.53	0.02	1.14	-0.77	6.06	0.02	1.27	-1.68	3.30	0.02	1.18	-1.85
	L3	Front.	2.86	0.02	1.11	0.06	3.79	0.02	1.29	-1.25	2.41	0.02	1.28	-1.14
	L5	Front.	0.71	0.02	0.83	1.07	0.95	0.02	1.24	0.32	0.68	0.01	2.13	-0.03
	Lumbar	Front.	1.91	0.02	1.05	0.44	2.43	0.02	1.29	-0.53	1.56	0.02	1.37	-0.70
	Thoracic	Front.	3.18	0.02	1.14	0.50	7.84	0.02	1.20	1.95	3.17	0.02	1.19	-0.05
	Cervical	Front.	0.71	0.02	0.94	-3.63	2.31	0.02	1.31	-2.21	0.69	0.01	1.84	-1.32
	Pelvis	Front.	0.43	0.02	-0.49	-0.06	2.76	0.02	-1.68	0.65	1.59	0.02	-1.85	-0.33